ABSTRACT

Title of dissertation: EFFECTS OF GALLIUM-DESFERRIOXAMINE COMPOUNDS ON BACTERIA

Mohammad Ahmed, Emily Brode, Thomas Brown, Somayah Eltoweissy, Stephanie Gross, Seth Markowitz, Michael McCutchen, Reed Portney, Jacob Reinhart, Cristian Salgado,Melissa Walsh, Sean Wassel

Mentor: Ben Woodard
Biotechnology Research and Education Program

Over 70% of nosocomial infections in the United States are resistant to one or more traditional antibiotics, necessitating research for alternative treatment options. This study aims to chelate gallium (Ga) onto a bacterial siderophore, desferrioxamine (DFO), to retard bacterial growth. By exploiting natural bacterial pathways, metal-siderophore treatments are hypothesized to circumvent traditional resistance mechanisms. Additionally, the GaDFO complex will be tested against several bacterial species to determine the specificity of DFO uptake. This research aims to prove the feasibility of siderophore piracy as an alternative to antibiotics. In showing the feasibility of siderophore piracy mechanisms, this research will enable the development of future avenues for protecting against resistant nosocomial infections.

Effects of Gallium-Desferrioxamine Compounds on Bacteria

Team Silver

Mohammad Ahmed, Emily Brode, Thomas Brown, Somayah Eltoweissy, Stephanie Gross, Seth Markowitz, Michael McCutchen, Reed Portney, Jacob Reinhart, Cristian Salgado, Melissa Walsh, Sean Wassel

Mentor: Ben Woodard

Thesis submitted in partial fulfillment of the requirements of the Gemstone Program, University of Maryland, 2015

Advisory committee:

Dr. Frank Coale. Gemstone Program Director

Dr. Kristan Skendall.

Mr. Ben Woodard

Mr. John Kerwin

Dr. David Rozak

Dr. Andrew Lees

Ms. Marybeth Shea

Dr. Steve Hutcheson

Acknowledgments

Team Silver would like to thank the following individuals and organizations for their support and contributions:

Ms. Nedelina Tchangalova for serving as the team's librarian

Dr. David Rozak for assisting in the review of the thesis proposal

Dr. John Buchner, for providing the team with bacteria strains for experiments

Kevin Knapstein, for hosting the team in the UMD Bioprocess Scale-Up Facility

John Kerwin, for hosting the team at the UMD Biopharmaceutical Advancement Facility

All the staff of the UMD BSF and BAF, including Jahmal D. Rich, Jeffrey Clark, Joseph Ecker, Nicholas Pellegrino, Chase Siegel

And the ACCIAC grant for funding this project

Table of Contents

Effects of Gallium-Desferrioxamine Compounds on Bacteria

The prevalence of antibiotic resistant bacteria is a major public health concern in society today. Over 70% of nosocomial infections in the United States have gained resistance to at least one antibiotic traditionally used in treatment (Lara, Ayala-Núñez, Turrent, & Padilla, 2009). Methicillin-resistant *Staphylococcus aureus* (MRSA) is alone responsible for 94,000 infections and 18,000 worldwide deaths annually (Mole, 2013). Antibiotics interfere with bacterial growth or survival and are often produced from natural products rather than synthetic, laboratory-engineered pathways. The use of antibiotics is known to contribute to the development of antibioticresistance, indicating that repeated or symptomatically prescribed usage may be causal factors in the evolution of resistance. Antibiotics have also been used as growth promoters in livestock, further contributing to the emergence of antibiotic-resistance (Mole, 2013). Continued overuse of antibiotics in the medical and agricultural settings have led to the increase in the presence of antibiotic resistance.

Bacteria utilize many different resistance mechanisms against antibiotics. Some bacteria block the antibiotic from binding with bacterial ribosomes and thus preserve protein synthesis. Intracellular/extracellular enzymatic degradation of the antibiotic can additionally lead to bacterial resistance (Benveniste & Davies, 1973). Alternatively, bacterial efflux pumps used by bacteria to excrete various compounds remove antibiotics before they can take effect (Van Bambeke, Balzi, & Tulkens, 2000). These pumps are relevant in regard to bacterial antibiotic resistance because antibiotic export via these

efflux pumps is becoming more common. Given the multitude of resistance mechanisms utilized to circumvent traditional antibiotics, research has focused on other antimicrobials to help combat the emergence of antibiotic-resistant bacteria. The World Health Organization (2014) publicized the need for developing new methods to circumvent the growing resistance problem worldwide in "Antimicrobial Resistance: Global Report on Surveillance." This report outlines the severity of the antibiotic resistance problem and suggests that immediate action must be taken to prevent the problem from growing.

Current approaches to solving bacterial resistance involve identifying and synthesizing new antibiotics. An example of these new methods can be seen in early 2015 as a new antibiotic, teixobactin, was isolated using *in situ* methods to cultivate previously uncultured microorganisms (Ling et al., 2015). Outside of new organisms, another avenue for combating drug resistant bacteria involves utilizing metal nanoparticles and ionic metals for their antimicrobial properties.

The use of metals for preservative and healing properties dates to ancient times and the antimicrobial effects of metals are still utilized today. New metal-based treatments are under consideration as well: nanoparticles are an attractive alternative to antibiotics due to the large range of targets to interact with although there is a risk associated with using nanoparticles (Rai, Yadav, & Gade, 2009). Nanoparticles may precipitate and harm the mammalian host (Braydich-Stolle, Hussain, Schlager, & Hofmann, 2005; Morones et al., 2005). Based on these findings, metal nanoparticles are a possible new avenue for antibiotic research, but not without potential pitfalls.

This study aims to find an effective method of delivering toxic ions into bacteria and thereby contribute to research on treatment of antibiotic resistant bacteria strains.

Ideally, a treatment would deliver toxic ions into the cytoplasm, circumventing traditional mechanisms of resistance. One potential chassis for such a treatment is a siderophore. Siderophores are iron-chelating molecules secreted by bacteria in iron-poor environments, such as the human body, to mobilize iron for the purpose of nourishing the bacteria (Beasley, Marolda, Cheung, Buac, & Heinrichs, 2011). Identifying a metal that can take place of iron and have toxic effects could yield results that exploit existing bacterial biochemical pathways for antimicrobial purposes.

Chitambar (2010) suggests that gallium compounds can interfere with iron uptake and enzymatic activity, thereby inhibiting growth of certain bacteria. To investigate the bactericidal and bacteriostatic effects of gallium chelated to siderophores, this experiment will analyze the effects of desferrioxamine-gallium (GaDFO) ligands on a number of bacterial strains. Desferrioxamine (DFO) is a commercially available siderophore that is naturally produced by several *Streptomyces* species (Seipke, 2015). DFO has been used in clinical settings to treat iron poisoning in infants without adverse effects (Jagobs, Greene, Gendel,1965). Based on this information, this study will address two main questions:

1. How does the GaDFO complex compare to traditional antibiotics in preventing bacterial growth?
2. Is the GaDFO treatment a broad-spectrum treatment or species-specific?

The aim of this research is to study if in an iron poor environment, DFO will form a complex with gallium and deliver the toxic ion to a bacteria to disrupt vital cellular functions. Many bacteria possess the genetic capacity to express different siderophore

receptors (Rabsch, Voigt, Reissbrodt, Tsolis, & Bäumler, 1999). As a result, the GaDFO complex may have broad spectrum capabilities.

Literature Review

Antibiotic History

Antibiotics are classified based on their chemical structure. The most common antibiotic structures are: β-lactams, macrolides, tetracyclines, fluoroquinolones, sulfonamides, aminoglycosides, imidazoles, peptides, and lincosamides. Antibiotics within a chemical structure group have a similar level of effectiveness, toxicity, and side effects. Penicillin and cephalosporin, for example, are both β-lactam antibiotics and have similar chemical structure with a four-membered, nitrogen-containing β-lactam ring at the core of the structure. The β-lactam ring in the chemical structure will attach to the active site of autolytic hydrolases to kill the bacteria. Kohanski, Dwyer, & Collins (2010) reviewed common antibiotics, their mechanisms of action, and which bacterial species they are effective against (see Table 1).

Drug type	Drug	Derivation	Species range	Primary target	Pathways affected
Fluoroquinolones*					
DNA synthesis inhibitor	Nalidixic acid, ciprofloxacin, levofloxacin and gemifloxacin	Synthetic	Aerobic Gram-positive and Gram-negative species, some anaerobic Gram-negative species (*C. perfringes*) and *M. tuberculosis*	Topoisomerase II (DNA gyrase), topoisomerase IV	DNA replication, SOS response, cell division, ATP generation, TCA cycle, Fe–S cluster synthesis, ROS formation, and envelope and redox-responsive two-component systems
Trimethoprim–sulfamethoxazole					
DNA synthesis inhibitor	Co-trimoxazole (a combination of trimethoprim and sulfamethoxazole in a 1:5 ratio)	Synthetic	Aerobic Gram-positive and Gram-negative species	Tetrahydrofolic acid synthesis inhibitors	Nucleotide biosynthesis and DNA replication
Rifamycins					
RNA synthesis inhibitor	Rifamycins, rifampin and rifapentine	Natural and semi-synthetic forms of ansamycins (derived from *S. mediterranei*)	Gram-positive and Gram-negative species, and *M. tuberculosis*	DNA-dependent RNA polymerase	RNA transcription, DNA replication and SOS response
β-lactams*					
Cell wall synthesis inhibitors	Penicillins (penicillin, ampicillin, oxacillin), cephalosporins (cefazolin, cefoxitin ceftriaxone, cefepime) and carbapenems (imipenem)	Natural and semi-synthetic forms of carbonyl lactam ring-containing azetidinone molecules (from *P. notatum*, *C. acremonium* and *S. cattleya*)	Aerobic and anaerobic Gram-positive and Gram-negative species	Penicillin-binding proteins	Cell wall synthesis, cell division, autolysin activity (regulated by LytSR–VncRS two-component system), SOS response, TCA cycle, Fe–S cluster synthesis, ROS formation, and envelope and redox-responsive two-component systems
Glycopeptides and glycolipopeptides					
Cell wall synthesis inhibitor	Vancomycin; teicoplanin	Natural and semi-synthetic forms of amino sugar-linked peptide chains (for glycopeptides) or of fatty acid-bearing, amino sugar-linked peptide chains (for glycolipopeptides) derived from actinobacteria	Gram-positive species	Peptidoglycan units (terminal D-Ala-D-Ala dipeptide)	Cell wall synthesis, transglycosylation, transpeptidation and autolysin activation (VncRS two-component system)
Lipopeptides					
Cell wall synthesis inhibitors	Daptomycin and polymixin B	Natural and semi-synthetic forms of fatty acid-linked peptide chains (from *S. roseosporus* and *B. polymyxa*)	Gram-positive species (daptomycin), Gram-negative species (polymixins)	Cell membrane	Cell wall synthesis and envelope two-component systems
Aminoglycosides					
Protein synthesis inhibitors	Gentamicin, tobramycin, streptomycin and kanamycin	Natural and semi-synthetic forms of amino sugars (-mycins from *Streptomyces* spp. and -micins from *Micromonospora* spp.)	Aerobic Gram-positive and Gram-negative species, and *M. tuberculosis*	30S ribosome	Protein translation (mistranslation by tRNA mismatching), ETC, SOS response, TCA cycle, Fe–S cluster synthesis, ROS formation, and envelope and redox-responsive two-component systems
Tetracyclines					
Protein synthesis inhibitors	Tetracycline and doxycycline	Natural and semi-synthetic forms of four-ringed polyketides (from *S. aureofaciens* and *S. rimosus*)	Aerobic Gram-positive and Gram-negative species	30S ribosome	Protein translation (through inhibition of aminoacyl tRNA binding to ribosome)
Macrolides					
Protein synthesis inhibitors	Erythromycin and azythromycin	Natural and semi-synthetic forms of 14- and 16-membered lactone rings (from *S. erythraea* and *S. ambofaciens*)	Aerobic and anaerobic Gram-positive and Gram-negative species	50S ribosome	Protein translation (through inhibition of elongation and translocation steps) and free tRNA depletion
Streptogramins					
Protein synthesis inhibitors	Pristinamycin, dalfopristin and quinupristin	Natural and semi-synthetic forms of pristinamycin I (group B, macrolactone ringed-peptides) and pristinamycin II (group A, endolactone oxazole nucleus-bearing depsipeptides) (from *Streptomyces* spp.)	Aerobic and anaerobic Gram-positive and Gram-negative species[‡]	50S ribosome	Protein translation (through inhibition of initiation, elongation and translocation steps) and free tRNA depletion
Phenicols					
Protein synthesis inhibitor	Chloramphenicol	Natural and semi-synthetic forms of dichloroacetic acid with an aromatic nucleus and aminopropanediol chain (from *S. venezuelae*)	Some Gram-positive and Gram-negative species, including *B. fragilis*, *N. meningitidis*, *H. influenzae* and *S. pneumoniae*	50S ribosome	Protein translation (through inhibition of elongation step)

*Drug efficacy can vary across species range based on drug generation. ‡When used as a combination of pristinamycin I and pristinamycin II. *B. fragilis*, *Bacillus fragilis*; *B. polymyxa*, *Bacillus polymyxa*; *C. acremonium*, *Cephalosporium acremonium*; ETC: electron transport chain; *H. influenzae*, *Haemophilus influenzae*; *M. tuberculosis*, *Mycobacterium tuberculosis*; *N. meningitidis*, *Neisseria meningitidis*; *P. notatum*, *Penicillum notatum*; ROS, reactive oxygen species; *S. ambofaciens*, *Streptomyces ambofaciens*; *S. aureofaciens*, *Streptomyces aureofaciens*; *S. cattleya*, *Streptomyces cattleya*; *S. erythraea*, *Saccharopolyspora erythraea*; *S. mediterranei*, *Streptomyces mediterranei*; *S. pneumoniae*, *Streptococcus pneumoniae*; *S. rimosus*, *Streptomyces rimosus*; *S. roseosporus*, *Streptomyces roseosporus*; *S. venezuelae*, *Streptomyces venezuelae*; TCA, tricarboxylic acid.

Table 1. A review of common classes of antibiotics and their characteristics.

Bacterial Resistance

Overuse of antibiotics for medical and agricultural purposes has contributed to the bacterial ability to circumvent susceptibility to treatments. The WHO (2014) published a global report to evaluate the magnitude of antimicrobial resistance on a global scale.

Resistance is most prevalent in MRSA, the most common cause of postoperative infection. It first emerged in hospitals during the 1960s and the incidence of community-acquired MRSA has increased dramatically since then (Baba et al., 2002). Infections range from 20-80% of populations in all WHO regions affected (WHO, 2014), illustrating the wide reaching detrimental effects of growing antibiotic-resistant microorganism. Vancomycin is one of the only treatment options for MRSA, however resistance to this last line of defense drug has increased since its emergence in the late 1980s (Appelbaum, 2006).

To find new treatment options, researchers turned to where antibiotics were originally discovered: in microorganisms. With 99% of microorganisms remaining uncultured *in vitro* (Rappé & Giovannoni, 2003), an enormous prospective pool exists from which new antibiotics can be isolated. Ling et al. (2015) isolated teixobactin, an antibiotic that inhibits bacterial cell wall synthesis, using a multi-channeled iChip device. The iChip device was designed to isolate a single bacterium from a diluted soil sample where the bacteria incubate in a natural environment, yielding a 50-fold increase in growth recovery than isolation from Petri dishes. Isolates from each well of the iChip were then taken and tested for antimicrobial action using plates overlaid with MRSA. Although ineffective against most Gram-negative bacteria, teixobactin was shown to be more effective in treating MRSA than the currently in place vancomycin treatments (Ling

et al., 2015). With the continued development of antibiotic resistance, the expansion of cultured bacteria using devices similar to the iChip may aid in the efforts of synthesizing new ways to treat infections.

Causes and Spread of Antibiotic Resistance

The development of antibiotic resistance involves selective pressure, mutation, and gene transfer. Selective (or evolutionary) pressures are environmental factors that may affect the reproductive success of an organism. An antibiotic can apply selective pressure by impeding bacterial growth and survival. Bacteria that carry genes that confer resistance to antibiotics are able to outlive the evolutionary pressure and replicate.

Martinez and Baquero (2000) have determined that there are three main types of genes whose products are important for the emergence of antibiotic-resistant mutants: genes involved in the synthesis and cell positioning of the antibiotic target, access of the antibiotic to the target, and protection of the target from the drug.

The phenotypic resistance of antimicrobials is stabilized and proliferated via horizontal and vertical gene transfer (HGT and VGT, respectively) between bacteria (Barbosa & Levy, 2000). VGT is indicative of survival-of-the-fittest proliferation of genomes from parental strains of bacteria, whereas HGT refers to the transfer of genes between organisms via non-traditional reproduction. HGT was first recognized in the transfer of virulence into a non-viral strain of *Corynebacterium diphtheriae* (Freeman & Morse, 1952), and has since been recognized as a method for the mutation and development of antibiotic resistance. Proliferation of resistance due to gene transfer increases the necessity for alternate methods to circumvent defenses against current antimicrobial treatments.

Mechanisms of Antibiotic Resistance

Enzymatic inhibition. Enzymatic inhibition occurs when bacteria neutralize antibiotic treatments before they can act on the target. β-lactams such as penicillin are among the most well documented antibiotics to which bacteria have developed this type of resistance. β-lactam antibiotics target transpeptidase enzymes responsible for cell wall synthesis by hydrolyzing the amide bond of the four-member β-lactam ring (Walsh, 2000). In Gram-negative bacteria β-lactamases are present in the periplasmic space, whereas Gram-positive bacteria excrete β-lactamase (Wilke, Lovering, & Strynadka, 2005). β-lactamase genes are incorporated into plasmids or transposons leading to the subsequent mobilization and transfer of genetic materials to other bacteria at a rapid rate. Further mutations to β-lactamase genes in these mobile elements can confer mechanisms for multidrug resistance including aminoglycosides, macrolides, sulfonamides and chloramphenicol.

Target site alteration. Target site alteration occurs when the gene products targeted by antibiotics are altered, preventing the normal interaction between the bacteria and the antibiotics. Ribosomes, both 50S and 30S, are major targets for antibiotics (Kohanski, Dwyer, & Collins, 2010). Erythromycin (and other macrolide antibiotics) function by binding to the 50S subunit and promoting the dissociation of peptidyl-tRNA from the ribosome, halting protein synthesis and cell growth (Menninger & Otto, 1982). 30S ribosome inhibitors, such as tetracycline, function by inhibiting the association of aminoacyl-tRNA and the bacterial ribosome, disrupting protein synthesis (Chopra & Roberts, 2001). These modifications allow the bacterial cells to maintain homeostasis despite the presence of the antibiotic. Similarly, if an antibiotic targets a protein that is

responsible for the synthesis of a growth factor that an auxotrophic bacteria can obtain from the environment, then the antibiotic will have no effect.

Membrane permeability shifts. The outer membrane bacteria is composed of phospholipids, lipopolysaccharides, and transport proteins embedded in the membrane. Under normal conditions, hydrophobic antibiotics (aminoglycosides, macrolides, rifamycins, novobiocin, fusidic acid, and cationic peptides) can permeate the outer membrane and enter the interior of the cell (Nikaido, 2003). Shifting membrane permeability involves changing the composition of the lipopolysaccharides core oligosaccharide. The composition of the core oligosaccharide is extremely variable, ranging from 6-10 monosaccharides. Bacterial strains have been found to be resistant to hydrophobic antibiotics when the full length of lipopolysaccharide is expressed (Delcour, 2009). These resistant strains exhibit a more tightly packed lipopolysaccharide layer in their outer membrane, inhibiting the permeation of hydrophobic antibiotics. Outer membrane permeability can also be changed by altering the porins embedded in the membrane. Porin channels present in the outer membrane enable small, hydrophilic antibiotics, such as β-lactams, tetracycline, chloramphenicol, and fluoroquinolones to enter the cell (Nikaido, 2003). Inhibiting transport across the porin channels decreases the effectiveness of the respective antibiotic.

Decreased membrane permeability is often accompanied by elevated levels of antibiotic efflux (Delcour, 2009). Drug efflux pumps have a loose substrate specificity allowing them to interact with a large range of drugs (Van Bambeke et al., 2000). While the precise mechanism for drug efflux is still debated, antibiotic efflux in conjunction with decreased membrane permeability creates a strong resistance system that can be

very difficult to overcome with traditional treatments.That is why our treatment will hope to utilize an existing pathway, which would further complicate the develop of a resistance mechanism in the bacteria.

Nosocomial Infections

History of nosocomial infections.

Drug-resistant strains of bacteria began to emerge in hospitals all over the world around the early twentieth century, concurrent with the development and emergence of antibiotic use. Soon after rapid utilization of these drugs during World War II, many military hospitals began to encounter sulphonamide (Levy & Marshall, 2004), penicillin, and streptomycin-resistant strains of bacteria (Levy, 1982). Between 1981 to 1995, the mortality rate from infectious disease increased by 4.8% annually in the United States, although the effects of infectious diseases have been reportedly more devastating in less developed countries worldwide (Cohen, 2000). Furthermore, rates of phenotypic antibiotic resistance continue to grow due to a variety of reasons. Despite the need for new treatments, pharmaceutical companies have focused on creating blockbuster drugs and subsequently the creation of new antibiotics has stagnated (Spellberg et al., 2008).

Types of nosocomial infections and breadth of populations affected.

Multidrug resistant bacteria pose a prominent threat to immunocompromised patients in hospitals as the proliferation within wards is facilitated by the susceptibility of these patients. In the United States, 40-60% of nosocomial outbreaks of *S. aureus* infections are MRSA, two-thirds of which occur in intensive care unit (Levy & Marshall, 2004). Though the current antibiotic treatment for MRSA is vancomycin, this drug may soon become ineffective as vancomycin-resistant strains of MRSA continue to emerge in

some states (Tenover et al., 2004). Without an effective treatment method, there could be a rise in fatalities attributed to MRSA and other drug resistant bacterial strains.

Gaynes et al. (1996) surveyed morbidity and mortality rates of neonates from 99 hospitals with high-risk nurseries. Bloodstream infections were the most common form of infection across all birth weights. The most common pathogens found amongst these infections were coagulase-negative staphylococci, which accounted for 58% of bloodstream infections observed and were most frequently associated with umbilical or central intravenous catheters.

Richards, Edwards, Culver, & Gaynes (1999) conducted a study of infections in pediatric intensive care units from 1992 to 1997 and found bloodstream infections to be the most commonly occurring at a rate 28% of the patients studied. Coagulase-negative staphylococci were the most common isolates from these infections followed by Gram-negative bacilli, most notably species of *Enterobacter*. Additionally, *Pseudomonas aeruginosa* was the most common species reported from cases of pneumonia and *Escherichia coli* were the most common isolates from urinary tract infections. The study concluded that these device-driven infections did neither correlate with length of stay in the hospital, number of hospital beds, nor season indicating the issue of infection was independent.

Kollef et al. (1997) aimed to establish the relationship between cardiac surgery patients, nosocomial infections, and the risk factors that contribute to infection. Out of the 607 cardiac surgery patients who were surveyed, 21.7% had subsequently acquired at least one nosocomial infection. Thirty patients died during their hospitalization and the study found an 11.5% mortality rate amongst patients with nosocomial infections, a

percentage significantly greater than the 3.2% of patients without nosocomial infections (Kollef et al., 1997). Although mortality rates have dropped since 1997 (Chen et al., 2012), strategies to prevent infection in high-risk patients undergoing cardiac surgery should be further developed.

Transmission: rates, pathways, preventative measures. One common pathway for bacterial infection in hospitals is transmission by direct contact. In an epidemiological survey that monitored bacterial transmissions, hand washing samples revealed that 30.8% of physicians and 16.6% of nurses had the presence of pathogenic bacteria on their hands (Bauer, Ofner, Just, Just, & Daschner, 1990). One study conducted across three intensive care units compared the efficacies of using the broad-spectrum antimicrobial agent, chlorhexidine, and 60% isopropyl alcohol with optional use of non-medicated soap. The study found that nosocomial infections were 25% less common when using chlorhexidine than when using isopropyl alcohol (Doebbeling et al., 1992). The data suggests that developing and implementing new hand washing agents and techniques can help reduce the risk of nosocomial infection related to direct-contact transmission without the need for additional antibiotic use.

An additional common mode of bacterial infection in hospital is device-related transmission. One study estimates that nearly 50% of nosocomial infections are device-related (Richards et al., 1999). The CDC (2004) recommended prophylaxis and antimicrobial-containing devices for the help reduce the risk of nosocomial infections associated with devices. However, two of the most common bacteria associated with devices, *P. aeruginosa* and *C. albicans*, have exhibited biofilm formation on the surfaces

of nearly all devices currently employed. Once formed, biofilms contribute to an increase in resistance to antibiotics (Pierce, 2005).

As the trend of resistance continues to grow, previously used methods begin to fail and make once manageable infections potentially life threatening. These growing patterns of multidrug resistance support the need for novel treatment options.

Metals as Antimicrobial Agents

The 19th century saw several significant contributions to the medicinal usage of metals. In 1852, Dr. J. Marion Sims developed silver sutures to close fistulas and silver catheters to divert urine during recovery periods (Sims, 1884). Dr. Carl Siegmund Franz Credé developed eye drops of 2% silver nitrate to prevent ophthalmia neonatorum in infants in 1881. Ophthalmia neonatorum affects up to 12% of all newborns. Similar eye drops were used for over a century and have dramatically reduced the incidence of ophthalmia neonatorum to 0.3% (Matejcek & Goldman, 2013). In the 19th and 20th centuries, scientists developed colloidal silver and silver nitrates for use in wound antisepsis and burn treatments. Researchers discovered that silver's antibacterial properties were due to silver ions. Through extensive research, they established that silver was an effective antimicrobial for over 650 species of unicellular organism (Alexander, 2009). Scientists examined the low concentrations at which metal ions were effective in preventing the growth of bacteria. Von Naegeli found that silver ions at a concentration of 9.2×10^{-9} M would kill *Spirogyra*, a freshwater bacterium (Russell & Hugo, 1994).

The medicinal applications of metals expanded in the 20th century. Silver foil was commonly used as a wound dressing. Colloidal silver was used in the treatment of corneal ulcers, interstitial keratitis, blepharitis, dacryocystitis, puerperal sepsis,

staphylococcal sepsis, tonsillitis, and acute epididymitis. The use of silver nitrate for the treatment of ophthalmia neonatorum spread worldwide. However, problems arose with the administration of colloidal silver. When administered orally, silver occasionally caused gastrointestinal problems; administered intravenously, it sometimes resulted in convolutions or death (Alexander, 2009). Although silver remained the most important medicinal metal, scientists used other metals to treat a variety of epidemics. Doctors administered tellurium, magnesium, arsenic, copper, and mercury to combat tuberculosis, leprosy, gonorrhea, and syphilis (Lemire et al., 2013).

The antimicrobial effects of metals were also used outside of the field of medicine. French mycologist Pierre-Marie-Alexis Millardet blended copper sulfate and slaked lime to prevent mildew from growing on grapes. This combination, known as the Bordeaux mixture, was used to prevent a variety of diseases in plants. Copper salts are commonly used in agriculture in developing nations and as organic agents in the United States and Europe (Lemire, Harrison, & Turner, 2013).

The toxicity of metal ions to mammalian cells is a potential concern surrounding the usage of metals to treat bacteria. Both the Ames test and *in vitro* micronucleus assay have been used to determine the genotoxicity of metal nanoparticles (Hartwig, 1995).

Siderophore Background

Iron is essential in many cellular pathways and as such interfering with iron uptake inhibits cellular proliferation. Miethke and Marahiel (2007) note that over 100 enzymes involved in metabolism utilize iron-containing cofactors, including iron-sulfur clusters or heme groups. Physiologically, the uptake of iron involves ferrous iron: Fe(II) and ferric iron: Fe(III). The redox reaction with Fe(II) and Fe(III) is reversible and

efficiently catalyzes biological redox and electron chain transfer reactions. The expression of genes required for iron acquisition and reactive oxygen species (ROS) protection is controlled by transcriptional and posttranscriptional regulatory proteins. These proteins interact with iron to detect the intracellular concentration of iron or the oxidation status and respond accordingly (Hantke, 2001).

Although iron is highly abundant, its ionic form is insoluble under physiological conditions and as such the sequestration and assimilation for microorganisms requires specific pathways. The first pathway utilizes the isolation of heme groups, which give hemoglobin and myoglobin the ability to bind oxygen because of the presence of iron atoms. These heme groups are extracted from the host organism's erythrocyte and serum hemoproteins supply. The second pathway involves the use of siderophores, high affinity iron-scavenging molecules. The affinity of siderophore chelation to iron ranges from 10^{12} to 10^{52} depending on its structure (Beasley & Heinrichs, 2010).

Ferrous iron is soluble when in a neutral aqueous solution and can be utilized by cells in this form. Fe(II) is commonly oxidized to Fe(III), through spontaneous reactions or by interactions with enzymes or oxygen in the host. This includes the commonly-occurring Fenton reaction: $Fe(II) + H_2O_2 \rightarrow Fe(III) + OH^- + OH^\cdot$ (Wardman & Candeias, 1996). Hydrogen peroxide reacts with free or not tightly bound Fe (II) to produce hydroxyl radicals and ferric iron. The ferric iron reacts with superoxides, known as an Haber-Weiss reaction, producing Fe(II) again: $O_2^{\cdot-} + Fe(III) \rightarrow O_2 + Fe(II)$ (Kehrer, 2000) allowing this redox reaction to continuously occur. Hydroxyl radicals are physiologically unsafe and ROS protection mediated by regulatory proteins or iron sequestration is vital.

Siderophores can be classified based on their internal chelating capabilities that enable iron wrapping, although high structural diversity exists within each of the classification groups. The two main classification variants are hydroxamates and phenal-catecholates, but carboxylate and pyoverdin siderophores also exist in smaller percentages. Bacteria assemble their siderophores through one of two pathways: non-ribosomal peptide synthesis (NRPS) and non-ribosomal peptide synthesis independent (NIS) (Beasley & Heinrichs, 2010; Liermann, Kalinowski, Brantley, & Ferry, 2000). The structure of siderophores, including a peptidic backbone and non-proteinogenic amino acid units, suggests that the ligands were initially NRPS and used as catalyzing antibiotics and other substances in Gram-positive bacteria (Crosa & Walsh, 2002). NIS siderophore assembly pathways utilize alternating dicarboxylic acid and amino acid building blocks; NRPS siderophores are synthesized as polypeptides (Barona-Gómez et al., 2006).

Iron-sensing activators and repressors control the expression of proteins that enable the assembly and export of siderophores. Siderophore production involves inhibition of ferric uptake regulatory (Fur) proteins and antisense RNA that act as repressors by interacting with iron (Fe^{2+}) under high-concentrations (Crosa & Walsh, 2002). Thus, a low-concentration of iron is necessary for the inhibition of Fur proteins and the production of siderophores. Fur protein homologues have been found in many bacterial species, making this a common sensor for siderophore production (Crosa & Walsh, 2002).

Once the siderophore sequesters iron from the environment, it must enter the bacterium through the outer membrane. In Gram-negative bacteria, the low permeability

of the outer membrane acts to prevent passive diffusion of foreign substances. As a result, the iron-siderophore complexes must cross the membrane through specific receptor mediated active transport. This active transport is dependent on specific outer-membrane receptors, periplasmic binding proteins, TonB complexes, and ATP-Binding Cassette (ABC)-type transporters (Ji, Miller, & Miller, 2012). TonB complexes are cytoplasmic energy-transducing protein complexes that facilitate membrane transport (Górska, Sloderbach, & Marszall, 2014). TonB-dependent receptors on the outer bacterial membrane achieve maximal transport efficiency at low concentrations of siderophore-ligand complexes. Active transport of the iron-siderophore complex pass the bacterial membrane through ATP hydrolysis and proton motive force (Moeck & Coulton, 1998). Like siderophores, TonB receptors are only expressed in iron-deficient environments. Recent studies have shown that the TonB receptor may allow siderophores produced by other bacteria to enter the cell, although it is highly specific to the diffusion of siderophores and not other compounds (Traxler, Seyedsayamdost, Clardy, & Kolter, 2012).

Although the cell walls of Gram-positive bacteria have strong metal-binding properties (Hu & Boyer, 1996), the ability to reabsorb the siderophore-iron complexes is problematic. Like Gram-negative bacteria, Gram-positive bacteria provide cytoplasmic entry of the small siderophore-iron complexes through active transport. In Gram-positive bacteria active transport is achieved by utilizing ABC transporters. The hydrolysis of ATP provides the necessary energy to move siderophore complexes across the bacterial outer membrane (Beasley & Heinrichs, 2010). The entire siderophore-iron complex must be within the cell before iron can be reduced from Fe(III) to Fe(II), releasing it from the

complex. Upon the release of iron, the siderophore may be recycled by the organism or degraded during a hydrolysis reaction accompanying the iron reduction. The fate of the siderophore varies depending on the specific organism (Liermann et al., 2000).

A secondary pathway of iron acquisition is an uptake capacity for siderophores secreted by different bacteria through a process called siderophore piracy (Traxler et al., 2012). Because iron is essential to the survival of the bacterium in the production of enzymes, the biosynthesis of macromolecules, and generation of energy the ability to sequester iron from the environment without the presence and expression of its individualized siderophore enables optimal live prognosis for the strains (Rabsch et al., 1999). The growth environment of bacteria can cause expression of both siderophore competition and piracy, therein changing the iron acquisition and subsequent gene expression within the organism (Traxler et al., 2012). Bacteria capable of siderophore piracy have receptors lining their outer membranes for siderophores that are not produced within the organism. These receptors allow for the secondary strategy by which bacteria can sequester free iron from the environment and feed. Some of the additional receptors are specific to certain siderophores secreted by another bacterium and some simply uptake other unrecognized substrates through the siderophore-receptor channels (Rabsch et al., 1999).

During infection the human body produces lactoferrin, a strong bacteriostatic agent. Lactoferrin acts to inhibit bacterial growth by limiting the amount of free iron available for pathogens or other infections. Depletion of free iron reserves slows the proliferation of pathogens or tumors. Siderophores bind iron with higher affinity than

lactoferrin or transferrin therein out-competing mammalian proteins during infection (Goetz et al., 2002).

Neutrophil Gelatinase-associated Lipocalin (NGAL) tightly binds with the catecholate-category ferric siderophores, showing little or no affinity to the hydroxamate-type, as a result limiting bacterial proliferation by depleting free iron. Unlike lactoferrin and interferrin, NGAL binds with a higher affinity to siderophore-marked iron as part of the innate immune system bacterial growth inhibition (Goetz et al., 2002). This mechanism explains how the body might protect against siderophore virulence and it is understood that NGAL mark the receptors on any catecholate-category siderophore. Although its affinity has only been found in one category of siderophores, its receptors have a non-specific capacity within the catecholate-type suggesting that all ferric siderophores maintain some nonspecific iron receptors. This abundance, of nonspecific outer membrane receptors, particularly seen in catecholate-type siderophores, helps to explain the ability of siderophore-piracy in iron acquisition through the use of nonspecific receptor channels of siderophores not produced by an organism.

Desferrioxamine, the focal point of this study, is a *tris*-hydroxamate siderophore whose molecular formula is given as $C_{25}H_{48}N_6O_8$. There are a variety of different structural organizations of desferrioxamine synthesized by strains of the *Streptomyces* species. Variants of desferrioxamine and related ferrirubin or ferrichrome structures each contain three hydroxamic acid groups, resulting in similar chemical and biological functions. Each structure is bound to different functional groups, explaining the individual similarity yet different interactions of the variates with their surrounding environments (Wong, Kappel, Raymond, Matzanke, & Winkelmann, 1983). The uptake capabilities of the

ferrioxamine variants are hypothesized to be controlled by the same importer systems. Desferrioxamine-B stimulates growth of mutant siderophores, xenosiderophores, which lack the cch and des gene clusters involved in coelicelin biosynthesis (Barona-Gomez et al., 2006). An additional mechanism has been proposed through which ferrioxamine siderophores may be taken up, specifically by *S. coelicolor*. This additional uptake pathway is selective for hydroxamate-containing complexes but allows xenosiderophores to be taken into the membrane. Both of these biosynthetic siderophore-uptake pathways have been reported for other bacterial species including *Bacillus anthracis, Erwinia chrysanthemi*, and *P. aeruginosa*. Three pathways of siderophore uptake are now known, each differing with the degree of selectivity to cognate siderophores, non-cognate siderophores, and xenosiderophore mutations (Goetz et al., 2002). These additional pathways are supportive of the feasibility of alternative route siderophore uptake as well as siderophore piracy mechanisms of both ligands secreted by other bacterial strains or siderophore-antibiotic chelated complexes.

By exploiting the siderophores' natural biochemical pathway to feasibly disguise treatments, the siderophore delivery system could circumvent traditional resistance mechanisms. An example of this siderophore mechanism is *Salmonella typhimurium* that produces enterobactin but also has receptors for FhuA, FhuE, and FoxA which are not secreted by the bacteria. Just as the siderophore is capable of binding to different metals, some bacteria express many different siderophore receptor types able to accept siderophores secreted by different bacteria allowing for a greater possibility of uptake and chelation nutrient sources. This uptake mechanism requires the secondary route of siderophore piracy (Rabsch et al., 1999).

Siderophores' Chelation of Metal Ions and (Conjugation to Antibiotics

Due to the chelating ability of siderophores, there has been interest in attaching toxic metal compounds and antibiotics to the ligand structure. Siderophore-antibiotic conjugates are capable of acting as antimicrobial delivery agents to bacterial cells while circumventing potential resistance pathways in Gram-negative bacteria (Ji, Miller, & Miller, 2012). *E. coli* and other species of *Enterobacteriaceae* produce microcins whose translocation across the outer membrane of Gram-negative bacteria is promoted by siderophore receptors (Morin et al., 2011; Vassiliadis, Destoumieux-Garzón, Lombard, Rebuffat, & Peduzzi, 2010). Although naturally occurring small antibiotic-siderophores, sideromycins, are cultivated and readily available (Raymond, Muller, & Matzanke, 1984), additional research is being done in the field of synthetic analogues to provide higher potency antibiotic-siderophore treatments.

Albomycin, a sideromycin produced by *Actinomyces subtropicus*, couples with a nucleoside analogue to cross the membrane through a peptide linker to effectively render the cell non-viable (Morin et al., 2011). Once the complex crossed the membrane barrier the linker must be hydrolyzed in the cytoplasm to initiate the nucleoside bactericidal properties. Within these natural mechanism pathways mutation and development of resistance is known to be quite rapid due transport system malfunction or loss of peptidase activity in the nucleoside analogue (Hartmann, Fiedler, & Braun, 1979). Salmycins are sideromycins produced by *Streptomyces violaceus*. Resistance develops in *S. Violaceus* through deletion of components of the siderophore uptake systems (Vértesy, Aretz, Fehlhaber, & Kogler, 1995). The research into xenosiderophore ligand complexes

has become a necessary step to circumvent the resistance developing by the use of sideromycins.

Siderophore-conjugates of fluoroquinolone, another popular class of antibiotics, have been investigated by several groups by introducing xenosiderophores including citrate, hydroxamate and pyochelin (Miller, McKee, Minnick, & Dolence, 1991). The antimicrobial activity was not greater than the parent antibiotic and in many cases activity was lost. A mechanism for release of the active principle, may also be needed for the efficient use of these synthetic analogues against their molecular targets. Construction of fluoroquinolone analogues with potential esterase and phosphatase cleavage sites that could result in increased and quicker release of the antibiotic were attempted but the results did not prove successful in synthesis.

β-lactam antibiotics have been intensively investigated as a potential antibiotic for siderophore ligand chelation, mostly in the exploitation of catechol isostere hydroxypyridone in monocyclic antibiotics (Dini & Aszodi, 2000). Monocarbamides showed poor efficacy in treatment of Gram-positive and high potency against Gram-negative bacteria. The ligand complexes may have several roles differentially impacting organisms based on the availability of transport routes, chelation affinity of the ligand's components, and significance of natural degradative resistance mechanisms (Page, Dantier, & Desarbre, 2010).

Siderophores of several classes of monocyclic β-lactam have been investigated. Monocyclic β-lactams showed generally poor activity against Gram-positive aerobic bacteria and anaerobic bacteria and high potency against Gram-negative bacteria. The three siderophore compounds were compared to isolated individual activity of aztreonam

(Zurenko, Truesdell, Yagi, Mourey, & Laborde, 1990). All three compounds exhibited enhanced activity against Gram-negative *P. aeruginosa* and *Stenotrophomonas maltophilia* but none of the monobactams exhibited significant inhibition of β-lactamases. The activating side chain of monocarbams is too bulky to fit readily into the active site of many β-lactamases and their hydrolytic efficiency is therefore significantly decreased (Zurenko et al., 1990).

All three compounds exhibited strong affinity for penicillin binding protein homologues in Gram-negative bacteria and were able to display the increased antibacterial activity despite the inhibitory ability towards β-lactamase activity (Han et al., 2010). Resistance to monocarbams was acquired quite readily in *E. coli* through loss of TonB receptors (Nikaido & Rosenberg, 1990). The siderophore-antibiotic complex was found to promote growth through their siderophore activity rather than inhibit it through their antibiotic activity.

Siderophore monobactams conjugates, in which a hydroxypyridone is carried on the oxyaminoacylamino side, were pursued, giving rise to a drug, PTX 2416 (Page et al., 2010). This monobactam showed enhanced activity, compared to aztreonam, toward Gram-negative bacteria especially toward *P. aeruginosa, Burkholderia cepacia*, and *Acinetobacter baumannii*. PTX 2416 is not as ineffective toward β-lactamases as the monocarbams proved to be and it was adjudged to play a role in β-lactamase inhibition.

Basilea Pharmaceutica has been investigating a series of siderophore monosulfactams (Page et al., 2010). Similar to all monocyclic β-lactams BAL30072, a product in early development, does not have major activity against Gram-positive but exhibits potent activity against most species of Gram-negative bacteria (Mushtaq,

Warner, & Livermore, 2010). Like most monocyclic β-lactams, BAL30072 is poorly hydrolyzed by class B β-lactamases and is an inhibitor of class C β-lactamases, evading resistance and increasing potency. The uptake mechanism remained intact as mutations in the TonB protein and siderophore receptors were infrequent and often ineffective. The overexpression of β-lactamases resulted in the most commonly encountered mechanism of acquired resistance (Page et al., 2010).

Antibiotic potency is lost when the natural combinations are chelated to siderophore complexes (Page et al., 2010). As effective transport mechanisms are a potential factor in the loss of potency, research is being encouraged to analyze the differential properties of certain siderophore-antibiotic chelated complexes. This has inspired research into finding metal ions that would be toxic to the bacteria and would not face problems in transport mechanisms due to size similarities to iron. The outer membrane of Gram-negative bacteria presents a most potent hurdle for many antibiotics in reaching their targets (Mushtaq et al., 2010). Therefore, there has been increased interest in using the natural iron-uptake mechanisms to mediate the entry of antibiotics into the cytoplasm. By attaching functional groups to antibiotics and siderophores, the receptors of the iron transport systems could be used to circumvent the bacterial membrane. Despite the effort put into synthesizing potential artificial and natural analogues, very few of the compounds have been successful. This could be credited to the decreased activity when compared to the parent antibiotics. There is also evolution of resistance due to the deletion of components involved in transport systems (Zurenko et al., 1990). However, such phenotypes appear to change depending on the organism used,

creating a need for new molecules and isolates to be investigated in relevant infection models.

Choosing Desferrioxamine

Desferrioxamine (DFO) is categorized as a *tris*-hydroxamate siderophore composed of alternating dicarboxylic acid and diamine or alkanolamines linked by amide or ester bonds and forming strong hexadentate complexes with ferric iron synthesized by the NIS pathway (Barona-Gómez, Wong, Giannakopulos, Derrick, & Challis, 2004; Challis, 2005). All three siderophore uptake mechanisms discussed earlier are able to uptake DFO, although each system's selectivity and specificity for siderophores and mutated xenosiderophores varies (Barona-Gómez et al., 2004).

DFO is widespread in nature and has several analogous forms produced and secreted by diverse species of bacteria (Yamanaka et al., 2005). Some of the most commonly synthesized desferrioxamine derivatives include desferrioxamine B, desferrioxamine E, and desferrioxamine G (Figure 1). Although there is great diversity, most DFO compounds are synthesized in four steps. First, L-lysine is decarboxylated by an enzyme similar to PLP-dependent amino acid decarboxylases (DesA) yielding a molecule called cadaverine. Second, cadaverine is hydroxylated by an FAD-dependent amine monoxygenase (DesB) and converted into N-hydroxycadaverine. Third, a proposed acyl CoA-dependent acyltransferase (DesC) produces a hydroxamic acid from N-hydroxycadaverine. Finally, three hydroxamic acid intermediates are joined together and cyclized accordingly by DesD, a hypothetical protein (Barona-Gómez et al., 2004).

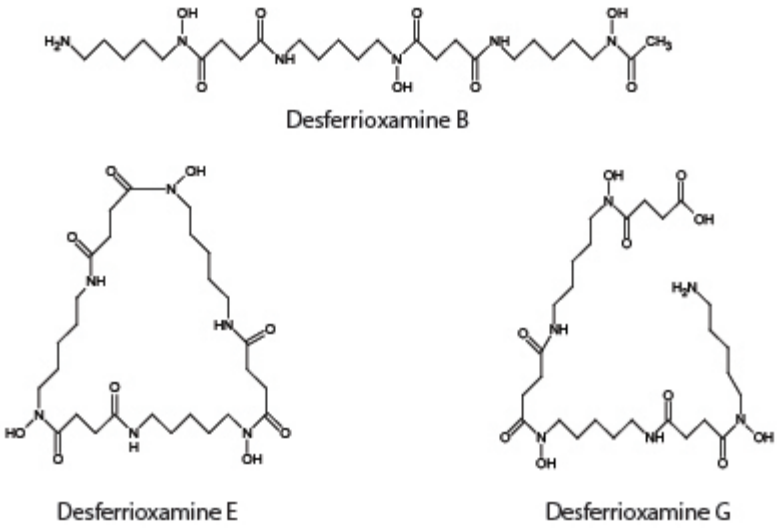

Figure 1. Common desferrioxamine derivatives found in nature: desferrioxamine B (Yamanaka et al., 2005), desferrioxamine E (Yamanaka et al., 2005), and desferrioxamine G (Bentley et al., 2002).

Tear lipocalin (Tlc) is a siderophore binding protein originally discovered in human tears. Tlc, also known as lipocalin 1 or von Ebners gland protein, is most commonly found in epithelial tissues (Miethke & Marahiel, 2007). The binding pocket of Tlc is approximately 15 Å and associates with hydrophobic ligands and siderophores including catecholates (enterobactin), hydroxamates (desferrioxamine B, rhodotorulic acid, TAFC, coprogen, ferrichrome, and ferricrocin), and mixed citrate-hydroxamates (aerobactin) (Fluckinger, Haas, Merschak, Glasgow, & Redl, 2004; Miethke & Marahiel, 2007). The dissociation constants for siderophore-iron sources of fungal uptake systems are similar to their Tlc affinities and potentially prevent the uptake of fungal Fe-hydroxamate siderophores. Reports show that Tlc does not significantly bind to bacterial siderophores such as ferrioxamine B with a great enough affinity to disrupt siderophore uptake systems. Siderocalin (also known as uterocalin, lipocalin 2 [Lcn2], NGAL, or 24p3) is a ligand binding protein found in acute-phase protein in mammals (Flo et al., 2004). Lcn2 competes with the high-affinity uptake system for *tris*-catecholates and

carboxy-mycobactins but does not provide significant defense against DFO as a hydroxamate siderophore.

The mesylate salt of DFO-B is commercially available, making it an attractive treatment component. Clinical applications have included the use of DFO-B for the treatment of iron overload in humans, specifically the product "Desferral" by Novartis. Two effects of DFO have been observed in pathogenesis: growth stimulation of the pathogen and immunosuppression of the host (Schubert & Autenrieth, 2000). High-level pathogenicity of *Yersinia enterocolitica* is attributed to the genes facilitating the uptake of ferrioxamine and using it as an iron source promoting virulence (Perry & Brubaker, 1979). Immunosuppression of the host due to the inhibition of T and B-lymphocytes proliferation, cytokine production of macrophages, and leukocytes is caused by DFO interference. Increased pathogenicity of *Y. enterocolitica* by DFO has been repeatedly observed in mice causing fatal septicemia and shock (Autenrieth et al., 1994; Autenrieth, Bohn, Ewald, & Heesemann, 1995). Similar stimulatory effects by DFO have been observed with *Streptomyces* pathogenesis (Yamanaka et al., 2005). Studies indicate a lessened virulence and immunosuppression by DFO-G, although its binding capacity is comparable to DFO-B (Autenrieth et al., 1994). DFO bound to hydroxyethyl starch (HES) can also be used instead for clinical DFO therapy. Studies indicate that usage of HES-DFO significantly decreased systemic oxidant injury and causes lessened toxicity levels in the lungs and kidneys observed in early sepsis while preserving the iron binding strength of DFO (Schubert & Autenrieth, 2000).

Using Gallium

Toxicity to bacterial strain and mammalian cell viability during treatment are essential components of a treatment. Gallium was ultimately chosen for its bactericidal genotoxic capabilities. Gallium nitrate, which dissociates into gallium and nitrate ions when placed in water, has shown antineoplastic activity when treating certain kinds of cancer. In addition, gallium acts as an immunosuppressant and anti-inflammatory agent (Chitambar, 2010). Concentrations as low as 10 μM $Ga(NO_3)_3$ inhibited growth of *P. aeruginosa*. Flooding iron particles into solution reversed this growth inhibition. Through this successful reversal of growth inhibition, gallium was shown to be a cause of iron metabolism disruption (Kaneko, Thoendel, Olakanmi, Britigan, & Singh, 2007).

To understand the effect of gallium within the bacterial cell it is necessary to look at the atomic qualities of the present ions. Gallium is a cation with a charge of 3^+, similar to the charge iron ions have when bound to desferrioxamine. Additionally, gallium and iron have similar ionic radii, 135 and 126 pm respectively in their nonionized states, and contributions to ionic bonding (Bernstein, 1998). Gallium's similarity to iron may explain why it is able to disrupt iron metabolism so readily; however, gallium cannot be reduced from a 3^+ ion to a 2^+ ion under physiological conditions while iron can readily reduce to a 2^+ ionic form and later be reoxidized back to its 3^+ state (Bernstein, 1998). Ga (III) and Fe (III) have equivalent binding constants and as such their differential affinity can be mediated based on relative availability of nutrient source. The availability of gallium is an ineffective inhibitor of any process which binds Fe^{2+} instead of Fe^{3+}, since Ga (III) is not oxidized physiologically.

Gallium has similar properties to ferric iron in both atomic radius and ionic charge, although it shows a 300-fold less affinity. The differential binding affinity can be compensated for by manipulating the concentrations of gallium in solution. The linear free energy relationship between Fe(III) and Ga(III) helps to explain the ability to use either metal as a chelating compound relatively interchangeably (Harris, 1983).

Mammalian Cell Relevance

To ensure the success of the proposed GaDFO treatment for potential in human-use, it is necessary to understand the effects of the treatment on mammalian cells. Divalent Metal Transporter 1, a duodenal mammal iron transport protein, is capable of transporting copper into HEK293 cells when those cells are deprived of iron (Jiang, Garrick, Garrick, Zhao, & Collins, 2013). This could imply that mammalian cells and other iron-chelating transporter proteins are capable of chelating other transition metals. Should the GaDFO treatments prove to be toxic to mammalian cells, the complexes would have no practical use in clinical settings.

Methodology

Bacterial Selection and Growth Conditions

Selection Criteria and Background Information. Biosafety level 1 and biosafety level 2 microbes were obtained from the American Type Culture Collection (ATCC) and the University of Maryland's Department of Microbiology. Bacteria were screened for their ability to synthesize a siderophore or produce a TonB-dependent siderophore receptor. These characteristics were determined using the UniProt database.

As TonB-dependent siderophore receptors are only present in Gram-negative bacteria, model selection was biased towards such organisms. Gram-negative microbes tend to be more resistant to antibiotics due to the presence of an outer membrane (Delcour, 2009), justifying this bias. Additionally, final selections were based on the clinical relevance of the bacterium, and ease of growth (i.e. simple growth media and short doubling time).

Selected organisms for this study were: *E. coli, S. aureus, Alcaligenes faecalis,* and *Enterobacter aerogenes.* Characteristics of each microbe are outlined on the following page:

Bacterium	Clinical Relevance	Siderophore Production/Siderophore Receptor
Escherichia coli	Common Gram-negative rod isolated from patients with bacteremia; responsible for 80% of community acquired urinary tract infections (Murray, Rosenthal, & Pfaller, 2009).	Naturally produces enterochelin siderophore, but certain clinical isolates also produce aerobactin. Can uptake siderophores it does not produce (Neilands, 1995)
Staphylococcus aureus	Responsible for a number of conditions such as Staphylococcal scalded skin syndrome, food poisoning, toxic shock syndrome, and skin infections (Murray et al., 2009).	Produces four siderophores: staphyloferrin A, staphyloferrin B, staphylobactin, and aureochelin (Reniere, Pishchany, & Skaar, 2010). Produces hydroxamate siderophore receptor (Dale, Doherty-Kirby, Lajoie, & Heinrichs, 2004).
Alcaligenes faecalis	Rarely associated with disease. However, opportunistic infections and fatalities in severely immunocompromised patients have been reported (Aisenberg, Rolston, & Safdar, 2004).	Production of hydroxamate and catecholate siderophores has been detected (Sayyed, 2006). UniProt analysis yielded at least three hypothetical TonB-Dependent siderophore receptors.
Enterobacter aerogenes	Historically associated with opportunistic infections in severely immunocompromised patients, and antibiotic resistance (Sanders & Sanders, 1997)	Produces aerobactin siderophore (Neilands, 1995). UniProt analysis yielded aerobactin receptors, and at least one hypothetical TonB-Dependent receptor.

Table 2. Characteristics of model organisms used in this study.

Experimental Growth Conditions. All microbes were grown in Luria Broth (LB) media (10 g tryptone, 10 g NaCl, and 5 g yeast extract per liter of diH_2O; plates had an extra 12 g of agar). Unless specified otherwise, organisms were incubated at 37 °C, and 250 RPM when shaking. Growth curve analysis was conducted to approximate mid-

log phase of all four bacteria in LB. Under conditions specified above, each microbe reached mid-log phase in the following time:

Bacterium	**Time Required to Reach Mid-Log Phase (Hours)**
Escherichia coli	5
Staphylococcus aureus	4
Alcaligenes faecalis	7
Enterobacter aerogenes	5

Table 3. Time required to reach mid-log phase. This table details model organism time requirements to reach mid-log phase. Data represents values of a single replicate. Since these experiments were carried out as a rough estimates, variance in growth times were carried out as a rough estimates, variance in growth times were not of particular concern.

The GaDFO treatment was compared to traditional antibiotics and controls to gauge the effectiveness of inhibiting bacterial growth. Controls included samples treated with diH_2O, and free gallium trichloride. Free gallium trichloride was used to evaluate differences in antibiotic delivery. To ensure antimicrobial activity of the GaDFO treatment was observed, a range of GaDFO concentrations between 0.5-500 μg/mL was used. This surpassed the clinically-relevant antibiotic concentration range of 0.008-4 μg/mL (Kelson, Carnevali, & Truong-Le, 2013).

CAS Assay

The chrome azurol S (CAS) assay is a metal indication assay used to detect unbounded iron ions. CAS is a compound which presents itself as a zwitterion when present in a strong acid solution. Figure 2 shows the structure of CAS before binding to free metal ions (Langmyhr & Klausen, 1963).

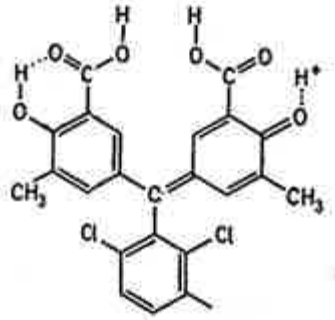

Figure 2. Structure of unbounded chrome azurol S (Langmyhr & Klausen, 1963).

When the CAS reagent is placed in a solution with a ligand that has a high binding potential (such as a siderophore) and free iron molecules, the subsequent reaction is notable. At first the iron will bond to the dye but eventually the stronger ligand will pull the iron from the dye changing its color from blue to red. This can be demonstrated by the following chemical equation: $FeDye^{3-\lambda} + L^{\kappa-} \rightarrow FeL^{3-\kappa} + Dye^{\lambda-}$ (Schwyn & Neilands, 1987). In this equation, Dye represents the chrome azurol S, Fe represents iron and L represents a ligand capable of pulling the iron away from the CAS, in this case our siderophore DFO-B. This equation is important to the experiments as similar binding is expected for gallium due to its similar charge and size to iron. The CAS assay is used in this study to determine if DFO can successfully binding to Ga in solution. The specifics of CAS assay are covered in the Appendix A2.

Microplate Fermentation

Microplate fermentation was used to determine the effect of treatment compounds. This technique is a convenient alternative to shake flask growth studies on bacteria (Hall, Acar, Nandipati, & Barlow, 2014). The primary concern with the use of a microplate is oxygen transfer into the media. Barrett, Wu, Zhang, Levy, & Lye (2010) demonstrated through CFD experiments that the microplate chassis is not inherently

limiting to gas transfer into the media or to mixing rate. The use of microplate readers is also viable with mammalian cells. Hoyer (2012) relates the effects of surface tension, density, kinematic viscosity, and well diameter to the minimum shaking frequency and amplitude required to break the surface of the liquid in each well, resulting in the following equation:

$$n_{min} = \sqrt{\frac{\sigma D_w}{4\pi V_F \rho d_0}} \quad (1)$$

where n_{min} is the minimum shaking frequency required for the force on the liquid to exceed the surface tension (σ); D_w is the well diameter, V_F is the filled volume of the well, ρ is the kinematic viscosity, and d_0 is the shaking amplitude (Hoyer, 2012). The V_F parameter varies for our experiments depending on the amount of reagents available at each time. While n_{min} only varies with the root of $1/V_F$, which is encouraging, if it is assumed that all plates were run at $n>n_{min}$, it is unclear what effect varying volume would have on the culture. The growth rate variable used for analysis was normalized against control trials under the same conditions (same plate, same V_F).

In the Biotek Synergy HT, the shaking amplitude is 0.0072in (0.19mm) and the shaking frequency on setting "3" is 19hz, where a cycle is three linear translations (Biotek Technical Support, personal communication, March 18, 2015). Thus, if a cycle is considered a single back-and-forth motion, the actual frequency is approximately 29hz. Assuming that the properties of the well are that of water, with a surface tension of 0.0741 N/m (Vargaftik, Volkov, & Voljak, 1983) and a density of 993.112 kg/L (Zimmerman, John, Trauthwein, Dingerdissen, & Huthmacher, 2003), the actual shaking frequency is comfortably above the minimum for V_F values of both 1 mL and 2 mL.

Different well volumes should divide out during analysis; there is no rational basis to assume V_F would affect treated and non-treated wells differently.

The use of microplate readers on mammalian cells is further discussed by Chaturvedi (Chaturvedi, Sun, O'Brien, Liu, & Brooks, 2014), who found that 24 deep-well plates had comparable characteristics to shake flask growth. The study also noted the importance of a confounding variable called "edge effects." Edge effects can refer to differing cell adhesion in wells that do not border four other wells (Tanner, n.d.) or to any difference in physical properties in wells on the edge of the plate versus the center. This can be addressed by heating the sides of the plate as well as the bottom, or by using a transparency microplate, in which the liquid is held in the center of the well, not in contact with the walls, and heat is therefore only transferred from the bottom of the plate into the liquid (Lau, Zahidi, Liew, & Ng, 2015).

A microplate reader is well suited to this project due to two factors: the ability to simultaneously run up to 24 samples (this experiment used a Biotek Synergy HT) and control for any deviations or confounds (e.g. temperature fluctuations) as they would be consistent across the whole experiment and affect the control simultaneously. Although there were no steps taken to mitigate the edge effects described by Lau et al. (2015), all microplate experiments were carried out for 24-48 hours at a steady temperature of 37°C. This period is assumed to be sufficient time for the plate to equilibrate. The final validation of this technique comes from its agreement with shake flask studies conducted in parallel, discussed below. Protocol A1 discusses microplate preparation and observation in more detail.

In this section, the term "experiment" refers to a set of microplate fermentations, which were performed simultaneously in the same microplate and on the same species of bacteria. The term "trial" refers to a single fermentation in a single well of the microplate, with a specific concentration of a treatment compound. Trials were always performed in triplicate to allow the calculation of the standard deviation. Treatments spanned four orders of magnitude in concentration (5.15×10^{-3} to 5.15×10^{-6} M), with two treatment options: GaDFO complex (with mesylate and chloride counterions) and "bare" Ga^{3+} ions (with chloride counterions). The 5.15×10^{-3} bare gallium treatment showed an intermittent and unknown reaction with the LB media and as such, this treatment level was not explored in all trials.

The direct response variable was measured by optical density as a function of time. Optical density is considered the benchmark measurement for cell growth and techniques are readily available as detailed by Woodard, Knapstein, and Barrett (2013). Each trial's growth curve was therefore fit to the function:

$$x(t) = A_0 + A_1 x + A_2 x^2 + A_3 x^3 + A_4 x^4 \quad (2)$$

Where x is the optical density of the culture at a 600 nm wavelength as reported by the plate reader. In some cases a fifth order polynomial was used instead. This function allowed the calculation of *dx/dt* for each well (the growth rate), and the maximum value for each well was normalized by dividing by the average maximum growth rate of the control

$$Maximum\ Normalized\ Growth\ Rate\ (MNGR)\ of\ well\ i$$

$$= \frac{\max\left(\frac{dx_i}{dt}\right)}{\left(mean\left(\max\left(\frac{dx_{controls}}{dt}\right)\right)\right)}$$

In cases where the growth rate was severely decreased (but non-zero), a prohibitively long experiment would be necessary to determine the final OD of each trial, so the rate was used instead for all analysis.

Influential variables on the growth curves were likely informed by temperature, nutrient content, inoculation CFU count, treatment concentration, oxygen transport into growth medium, and rotating pattern/rate. Potential sources for error include refraction due to condensation on the microplate lid, and treatment-media interaction. For the latter reason, the 5.15×10^{-2} M gallium treatment was omitted as the reaction with the media both increased the turbidity and potentially affected the nutritional content. The most important confounding variables were the relationship between optical density and colony forming units and the relationship between CFUs and toxin production (Woodard, Knapstein, & Barrett, 2013). The former was addressed with further experimentation and the latter would require specific methods not available with current resources.

Colony Forming Units (CFU) Analysis

CFU analysis was performed to verify the efficacy levels of treatment data collected from microplate fermentations on three organisms: *A. faecalis*, *E. aerogenes*, and *E. coli*. Bacteria were grown in LB to mid-log phase. Experimental and control growth media were prepared according to Protocol A3. Briefly, control media contained 1X LB, while experimental media had 1X LB plus 5.15×10^{-4} M GaDFO (and mesylate

and chloride counterions), or $5.15x10^{-4}$ M gallium trichloride. Experiments were performed in technical triplicates.

Once grown in LB until mid-log, treatment flasks were inoculated and grown to mid-log stage. After inoculated cultures reached mid-log, the incubation period was terminated. Samples were diluted and plated on LB agar according to Protocol A3. Plates were left to grow overnight at 37 ℃ and colonies were counted the following day.

Similarly, CFU analysis was used to determine antibiotic effectiveness against *E. aerogenes*, and *E. coli*. In this case, a known bactericidal (ampicillin) and a known bacteriostatic (chloramphenicol) were used as "ideal" antibiotics. Antibiotic concentrations used in these experiments were 1.0 g/10 mL for ampicillin, and 0.35g/10 mL for chloramphenicol. Concentrations choices were based on predetermined procedures used by the University of Maryland Bioprocess Scale-Up Facility.

Human Embryonic Kidney 293 Mammalian Cell Culture

The final phase of experimentation involved testing the GaDFO treatment in the presence of mammalian cells. To complete this phase within a time sensitive window, it was important to pick a cell line that was easily culturable and attainable. Human Embryonic Kidney cells supplied by the Biopharmaceutical Advancement Facility (Rockville, MD) were cultured in 1X DMEM media supplemented with 10% Fetal Bovine Serum, and 1% Penicillin/Streptomycin. Once growth reached 7,000 cells/cm^2, cells were mixed with 10^{-2} GaDFO stock and then incubated at 37℃ with 5% CO_2 for 20 hours with growing and confluent cells. After this incubation period, cells were counted using a hemocytometer.

Treatment Preparations & Compositions

For this and following sections, "GaDFO treatment" refers to gallium trichloride mixed with desferrioxamine-B mesylate before addition to the culture medium. "Ga treatment" refers to gallium trichloride added to the culture medium. For a table of treatment concentrations, consult Supplemental S3. Treatments were prepared in accordance with protocols from Appendix A depending on the nature of the experiment.

Computational Analysis of DFO Biosynthesis and Siderophore Receptors

DFO Biosynthesis. Phylogenetic analysis for DFO biosynthesis was completed based on DesA homology. The reference sequence used for analysis was taken from *Streptomyces coelicolor* an Actinomycete that produces desferrioxamine E (Bentley et al., 2002). The *S. coelicolor* DesA amino acid sequence (see Supplemental S1) was obtained from the Integrated Microbial Genomes (IMG; Markowitz et al., 2012) database. Protein Basic Local Alignment Search Tool (Altschul, Gish, Miller, Myers, & Lipman, 1990) was used to find organisms with potential DesA homologues. Criteria for reported microbes included:

1) An Expected (E) value less than 10^{-5} - indicating less than 0.00001 homologous proteins expected to show up as a positive hit due to chance alone. This parameter is dependent on the size of the input sequence and the size of the database in use.

2) A query coverage greater than 95% - indicating at least 95% of the reference sequence was aligned with the hit. For example, in this specific case the query sequence had 480 amino acids. A query coverage greater than 95% would indicate that all hits had at least a 456 amino acid region that aligned with the query.

3) Verification on the IMG server to ensure that the DesA gene (PLP-dependent amino acid decarboxylase) was followed by an FAD-dependent amine monooxygenase (DesB), an acyl CoA-dependent acyltransferase (DesC), and a hypothetical protein (DesD).

Bacteria were selected based on their representation of different phylogenetic classes. After compiling a list of DesA sequences, phylogenetic analysis was carried out using Multiple Sequence Comparison by Log-Expectation (Edgar, 2004) software using default parameters. The output file (Pearson/FASTA format) was analyzed and re-rooted using Dendroscope software (Huson & Scornavacca, 2012). Tree rooting was based on the class taxonomic level and the tree was prepared for presentation using Interactive Tree of Life software (Letunic & Bork, 2011).

Siderophore Receptors. Computational analysis of siderophore receptors was similar to the DFO biosynthesis methodology outlined above. First, a reference amino acid sequence from a desferrioxamine-B transporter was identified as described by Tanabe et al. (2005) (see Supplemental S1). Then, IMG and BLASTp software was used in tandem to search for homologous proteins in *A. faecalis, E. aerogenes, S. aureus,* and *E. coli*. This data was used to generate a possible explanation of the hypothesis as to why the GaDFO treatment did or did not work in varying bacterial strains. Criteria for proposing the presence of a homologous receptor protein included: an Expected (E) value less than 10^{-5}, a query coverage greater than 95%, and presence of an AraC transcriptional regulator gene directly upstream of the transporter. This last criterion was based on findings that an AraC-like protein is required for expression of the Desferrioxamine B transporter in *Vibrio vulnificus* (Tanabe et al., 2005).

Statistical analysis

One-way Analysis of Variance (ANOVA) was used to determine the statistically significant differences between treatment conditions. To accomplish this, a between-subjects one-way ANOVA was utilized, as each level of treatment condition was independent and unrelated to the other conditions with which it was compared. ANOVA was used to measure the CFU (DV) treatment comparisons of *A. faecalis, E. coli,* and *E aerogenous* against control, free gallium, GaDFO gallium, and in some cases, antibiotics (IV levels). The use of ANOVA also showed the maximum growth rates of bacteria grown during microplate fermentation MNGR (DV) as compared to control, free gallium, and GaDFO (IV levels). Each ANOVA was run using IBM SPSS software with an error margin of $\alpha = 0.05$.

Results

GaDFO CAS Assay

CAS assay plates were made following the protocols in Appendix A2. The plates were given 24 hours to equilibrate and then analyzed. First, a simple visual examination of the plates was done to ensure that a color gradient existed. The color changes from blue at the highest concentration of gallium ions (2.50×10^{-5} moles/L) to red when fewer gallium ions are present in solution.

Once the gradient was visualized, absorbances (A_{590}) were recorded using the Biotek Synergy HT plate reader and the results were plotted versus concentration of gallium (Figure 3).

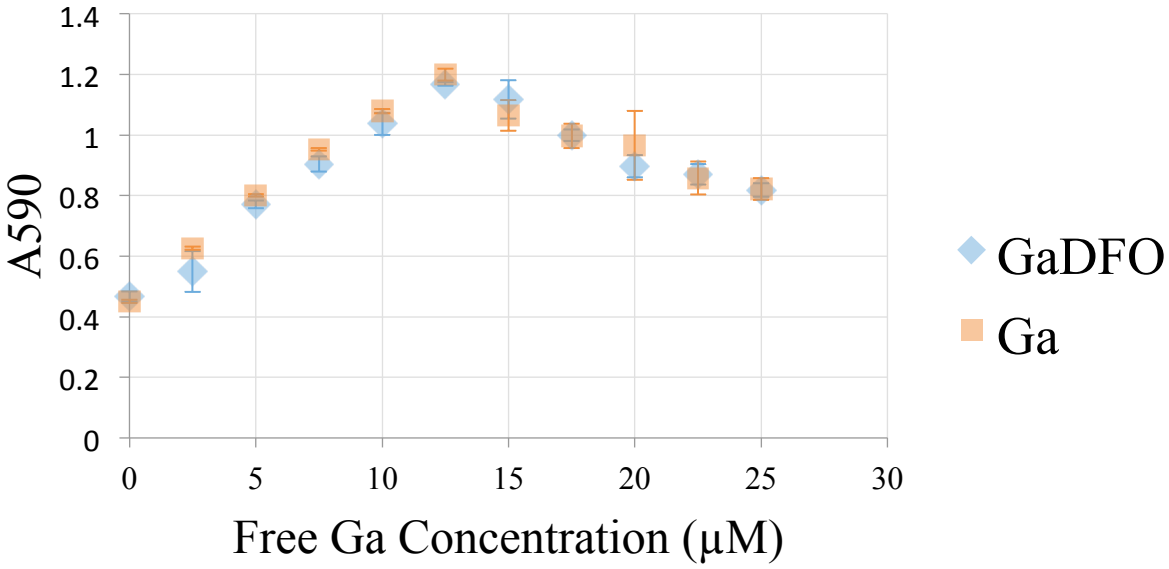

Figure 3. 0µM to 25µM concentration experimental plates of $GaCl_3$ and GaDFO complex respectively.

To determine the concentration of gallium ions expected to bond to CAS the following equations 3 and 4 were used.

$$[Ga_{CAS}] = \frac{[Ga_0]*V_{Ga}}{V_{tot}} \quad (3)$$

Equation 3 is used to determine the concentration of gallium bound to CAS ($[Ga_{CAS}]$) in the Ga CAS assay plates. $[Ga_0]$ is the concentration of the stock solution of gallium placed in the plate V_{Ga} is the volume of gallium added and V_{tot} represent the total volume the solution in the well.

$$[Ga_{CAS}] = \frac{[Ga_0]*V_{Ga}-[DFO_0]*V_{DFO}}{V_{tot}} \quad (4)$$

Equation 4 is used to determine the concentration of gallium bound to CAS ($[Ga_{CAS}]$) in the GaDFO CAS assay plates. $[Ga_0]$ is the concentration of the stock solution of gallium placed in the plate, V_{Ga} is the volume of gallium added to the well, $[DFO_0]$ is

the concentration of the stock solution of DFO, V_{DFO} is the volume of DFO added to the well, and V_{tot} represent the total volume the solution in the well.

Using equations 3 and 4, the ability of Ga to bind to the CAS reagent is demonstrated. This shows the ability of DFO to preferentially bind to Ga over CAS. When DFO and Ga are both present at concentrations of 25 μM in solution and mixed together with CAS they displayed a red color similar to the color given by a solution of plain DI water with no added metal ions. The DFO is bound to the gallium preventing it from binding to the CAS reagent which would create a blue color. Figure 3 depicts a 1:1 binding ratio between DFO and Ga shown by the overlapping of the Absorbance readings in the graph.

Microplate Results

Microplate fermentations show statistically significant differences between treated and untreated bacteria, as well as between Ga treated and GaDFO treated bacteria with a significance level of $\alpha = .05$. The response of *A. faecalis* to our treatment complexes is shown in Figure 4.

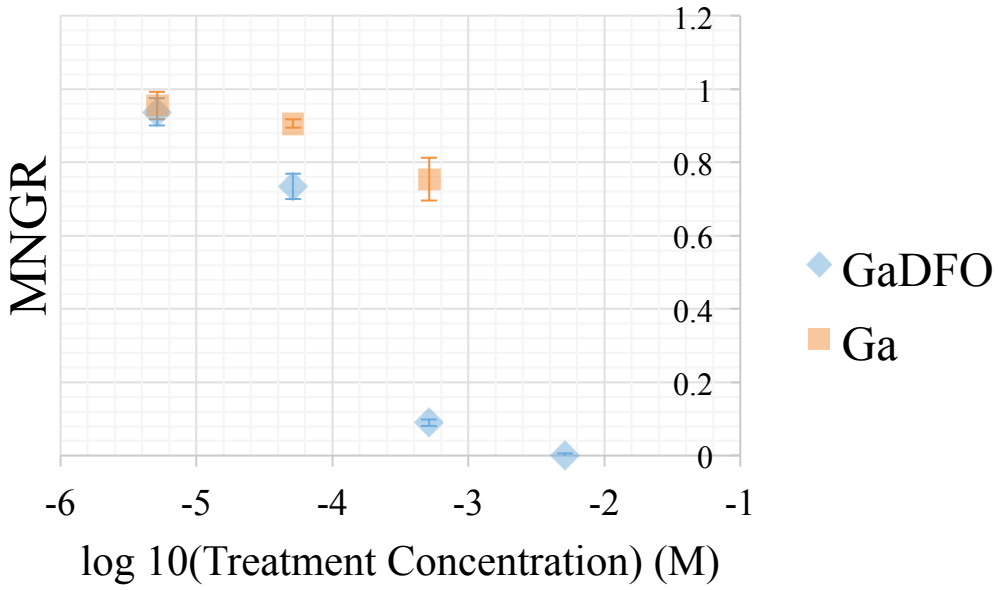

Figure 4. *A. faecalis* response to treatments. An early log-phase *A. facecalis* culture was transplanted from a shake flask into a microplate, starting OD600 0.3 (b = 1cm), and the continued growth was tracked for 24 hours.

A. faecalis showed a more dramatic response to the GaDFO complex than the Ga treatment, especially at higher concentrations. Notably, this species appears to be susceptible both the Ga and GaDFO complexes, even if there are differences in effectiveness.

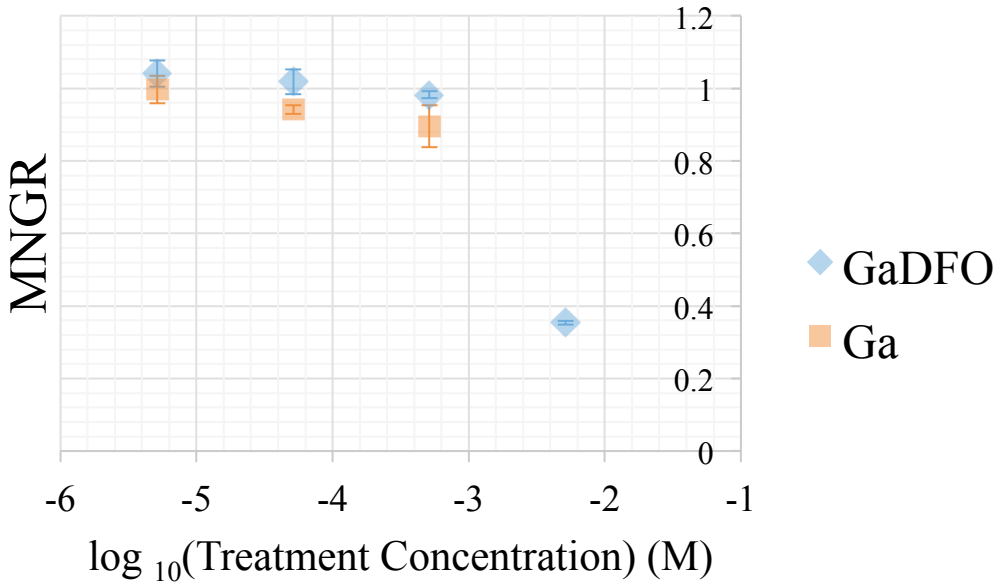

Figure 5. *E. aerogenes* response to treatments. An early log-phase *E. aerogenes* culture was transplanted from a shake flask into a microplate, starting OD600 0.3 (b = 1cm), and the continued growth was tracked for 24 hours.

E. aerogenes showed little response to the treatments overall (Figure 5). There was a statistically significant reduction in growth rate in the measurements of the highest GaDFO treatment level only.

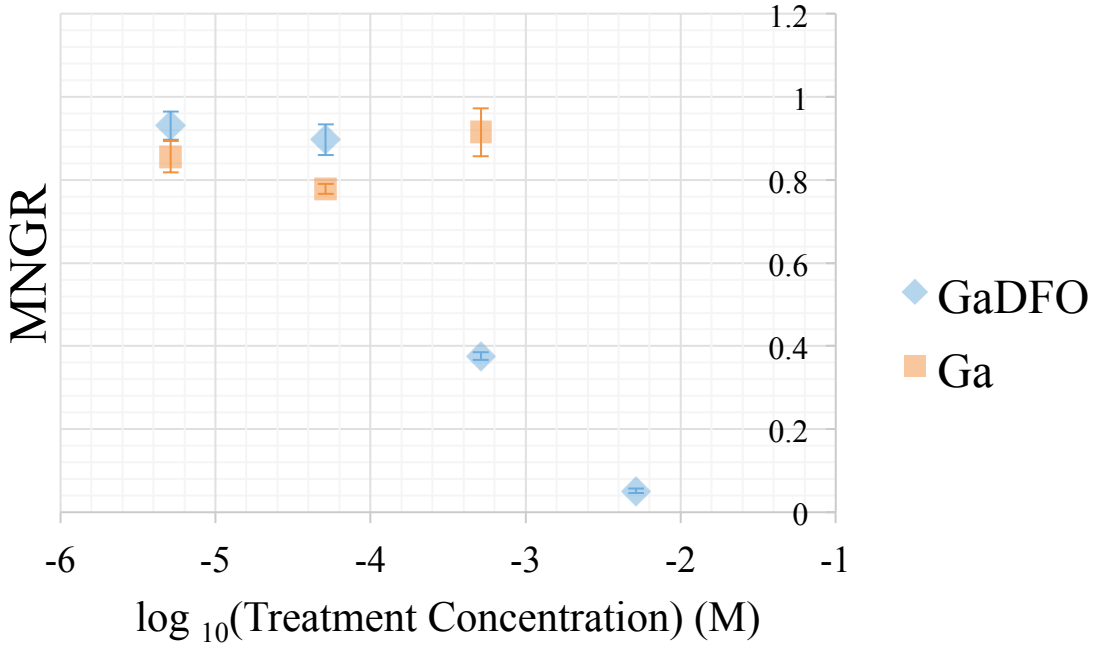

Figure 6. *E. coli* response to treatments. An early log-phase *E. coli* culture was transplanted from a shake flask into a microplate, starting OD600 0.3 (b = 1cm), and the continued growth was tracked for 24 hours.

Similar to the outcome of the trials for *A. faecalis,* there was an observed response to the GaDFO complex for *E. coli* (Figure 6), with growth nearly eliminated at the highest treatment level and some inhibition at the second highest level. The similarity ends there as *E. coli* did not respond to the free gallium ion treatment at any level.

S. aureus was also treated in a microplate using only stocks A and E, the highest concentrations of GaDFO and Ga respectively (see Protocol A1). In this instance gallium did not alter the nature of the media in any way noticeable by visual inspection, allowing the use of stock E. In cases where the media was considered unfit (previous experiments), it rapidly became and remained turbid after the addition of $GaCl_3$. With treatment concentrations of 5.15mM, the GaDFO complex yielded a maximum normalized growth rate of .203 *SD* = .0843 and the bare Ga ion gives a relative maximum growth rate of .550

SD = .0028. The procedure for fitting a polynomial to the *S. aureus* data also differed from previous trials as a different polynomial was used (5th order) but was otherwise the same. The use of a different polynomial is considered a non-issue because it is solely used for interpolation.

Statistical Significance of Microplate Results

Based on the results above, there was a distinct growth-inhibiting effect of the GaDFO complex at a 5.15 mM concentration consistent across four species, although not all were reduced to near-zero growth. The Ga treatments are not conclusive due to the lack of range, but tend to show less significant results than the GaDFO treatment.

Trial A		**Trial B**		
Type	[treatment] (M)	Type	[treatment] (M)	p value
GaDFO	5.15E-003	GaDFO	5.15E-004	0.000
GaDFO	5.15E-004	GaDFO	5.15E-005	0.000
GaDFO	5.15E-005	GaDFO	5.15E-006	0.000
GaDFO	5.15E-004	Ga	5.15E-004	0.000
GaDFO	5.15E-005	Ga	5.15E-005	0.000
GaDFO	5.15E-006	Ga	5.15E-006	0.768
GaDFO	5.15E-003	control	N/A	0.000
GaDFO	5.15E-004	control		0.000
GaDFO	5.15E-005	control		0.000
GaDFO	5.15E-006	control		0.000

Table 4. Statistical significance of microplate fermentation of *A. faecalis* in the presence of Ga and GaDFO treatments. Green boxes indicated a significant difference between the conditions on the X and Y-axes. Red boxes indicated a failure to reject H0 (that the treatments are no different). Boxes without numbers represent p = 0.000. Boxed treatments indicate important trials (adjacent trials of the same GaDFO concentration, trials where the Ga and GaDFO concentration are the same, and comparisons to the control).

As seen in Table 4, GaDFO treatments have clear statistical significance both between all levels of GaDFO treatment, and against equal concentrations of Ga treatments for *A. faecalis*. This implies that the presence of DFO (presumably in its bound state to Ga) increases the effectiveness of the Ga as an antimicrobial, and that these effects are concentration dependent.

Trial A		**Trial B**		
Type	[treatment] (M)	Type	[treatment] (M)	p value
GaDFO	5.15E-003	GaDFO	5.15E-004	0.000
GaDFO	5.15E-004	GaDFO	5.15E-005	0.000
GaDFO	5.15E-005	GaDFO	5.15E-006	0.000
GaDFO	5.15E-004	Ga	5.15E-004	0.000
GaDFO	5.15E-005	Ga	5.15E-005	0.020
GaDFO	5.15E-006	Ga	5.15E-006	0.265
GaDFO	5.15E-003	control	N/A	0.000
GaDFO	5.15E-004	control		0.000
GaDFO	5.15E-005	control		0.052
GaDFO	5.15E-006	control		0.346

Table 5. Statistical significance of microplate fermentation of *E. coli* in the presence of Ga and GaDFO treatments. Green boxes indicated a significant difference between the conditions on the X and Y-axes. Red boxes indicated a failure to reject H_0 (that the treatments are no different). Boxes without numbers represent p = 0.000. Boxed treatments indicate important trials (adjacent trials of the same GaDFO concentration, trials where the Ga and GaDFO concentration are the same, and comparisons to the control).

Reflected in Table 5, *E. coli* exhibits similar outcomes to *A. faecalis*. However, at low concentrations, the Ga and GaDFO treatments are indistinguishable. This may be in part due to a ceiling effect since both are very ineffective; there is limited room for difference between these two effects since a normalized average growth rate of 1 is (informally) a maximum. One of these compounds would have to actually increase the growth rate of *E.*

coli to show a statistically significant effect. A similar ceiling effect may occur at very high treatment levels as there is also a limited amount to which a culture can be inhibited (maximum normalized growth rate = 0).

Trial A		**Trial B**		
Type	[treatment] (M)	Type	[treatment] (M)	p value
GaDFO	5.15E-003	GaDFO	5.15E-004	0.000
GaDFO	5.15E-004	GaDFO	5.15E-005	0.935
GaDFO	5.15E-005	GaDFO	5.15E-006	0.996
GaDFO	5.15E-004	Ga	5.15E-004	0.178
GaDFO	5.15E-005	Ga	5.15E-005	0.284
GaDFO	5.15E-006	Ga	5.15E-006	0.848
GaDFO	5.15E-003	control	N/A	0.000
GaDFO	5.15E-004	control		0.999
GaDFO	5.15E-005	control		0.999
GaDFO	5.15E-006	control		0.893

Table 6. Statistical significance of microplate fermentation of *E. aerogenes* in the presence of Ga and GaDFO treatments. Green boxes indicated a significant difference between the conditions on the X and Y-axes. Red boxes indicated a failure to reject H_0 (that the treatments are no different). Boxes without numbers represent p = 0.000. Boxed treatments indicate important trials (adjacent trials of the same GaDFO concentration, trials where the Ga and GaDFO concentration are the same, and comparisons to the control.

E. aerogenes shows (Table 6) a marked lack of significance at all but the highest concentration of GaDFO treatment. There is a lack of evidence that the GaDFO treatment differs from the Ga treatment, because only the 515 mM GaDFO treatment showed any significant effect, and there is no comparable Ga treatment due to the issues with the media addressed above.

CFU Results

One-way ANOVA was conducted to examine the efficacy of treatment variants on CFU outcomes for *A. faecalis*, *E. aerogenes*, and *E. coli*.

A. faecalis. Three trials were run for each treatment condition: control, free gallium, and GaDFO. A significant effect was found between the treatments control ($M = 1.2\text{x}10^9$ CFU/mL, $SD = 5.8\text{x}10^7$ CFU/mL), free gallium ($M = 8.2\text{x}10^8$ CFU/mL, $SD = 2.3\text{x}10^7$ CFU/mL), and GaDFO ($M = 4.6\text{x}10^8$ CFU/mL, $SD = 1.2\text{x}10^8$ CFU/mL) with $F(2, 8) = 72.6$, $p < 0.00$. The interaction was probed using the Tukey HSD post hoc analysis (Table 7) to determine which factors added to the significant interactions between groups. Employing a 95% confidence interval, each measure of between groups testing was shown to be significant: control*gallium $p = 0.002$, control*GaDFO $p = 0.000$, gallium*GaDFO $p = 0.003$.

	Results		Comparison	
	Mean	SD	Trial A	Trial B
Control	1.23E+09	5.77E+07	Control	Ga
Ga	8.17E+08	2.31E+07	Control	GaDFO
GaDFO	4.60E+08	1.21E+08	Ga	GaDFO

Table 7. When looking at the *A. faecalis* CFU results, statistically significant results were reported when comparing the Ga and the GaDFO treatments to the control, as well to each other.

E. coli. Three trials were run of each treatment condition: control, free gallium, GaDFO, ampicillin, and chloramphenicol. Results indicated a significant effect between the treatment groups control ($M = 6.6\text{x}10^8$CFU/mL, $SD = 3.6\text{x}10^8$CFU/mL), free gallium ($M = 6.0\text{x}10^8$CFU/mL, $SD = 2.7\text{x}10^8$CFU/mL), GaDFO ($M = 4.5\text{x}10^8$CFU/mL, $SD = 4.9\text{x}10^8$CFU/mL), ampicillin ($M = 4.2\text{x}10^3$ CFU/mL, $SD = 2.7\text{x}10^3$ CFU/mL), and chloramphenicol ($M = 6.7\text{x}10^6$ CFU/mL, $SD = 6.6\text{x}10^6$ CFU/mL) $F(4, 17) = 3.8$, $p < 0.03$. The interaction was probed using the Tukey HSD post hoc analysis (Table 8) to

determine which factors added to the significant difference between groups. Employing a 95% confidence interval yielded the following interactions: control*gallium $p = 0.002$, control*GaDFO $p = 0.000$, control*ampicillin $p = 0.066$, control*chloramphenicol $p = 0.070$, ampicillin*chloramphenicol $p = 1.000$, ampicillin*gallium $p = 0.188$, ampicillin*GaDFO $p = 0.434$, chloramphenicol*gallium $p = 0.195$, chloramphenicol*GaDFO $p = 0.448$, gallium*GaDFO $p = 0.973$.

	Results		**Comparison**		
	Mean	SD	Trial A	Trial B	p value
Control	6.62E+08	3.62E+08	Control	Ga	0.999
Ga	6.03E+08	2.70E+08	Control	GaDFO	0.870
GaDFO	4.50E+08	4.86E+08	Ga	GaDFO	0.973
Control	6.62E+08	3.62E+08	Control	Amp	0.066
Amp	4.23E+03	2.70E+03	Control	Chlor	0.070
Chlor	6.70E+06	6.56E+06	Chlor	Amp	1.000

Table 8. When looking at the *E. coli* CFU results, statistically significant results were reported when comparing the Ga and the GaDFO treatments to the control, as well to each other

E. Aerogenes. Two separate tests were run for *E. aerogenes*, the first against a control, free gallium, and GaDFO treatment, and the second against a series of antibiotics. Results for *E. aerogenes* when tested against free gallium and GaDFO indicated no significant effect between the treatment groups control ($M = 1.0\text{x}10^{11}$ CFU/mL, $SD = 1.0\text{x}10^{11}$ CFU/mL), free gallium ($M = 1.8\text{x}10^{10}$ CFU/mL, $SD = 2.8\text{x}10^{10}$ CFU/mL), and GaDFO ($M = 2.1\text{x}10^{9}$ CFU/mL, $SD = 2.1\text{x}10^{8}$ CFU/mL) $F(2, 14) = 3.2$, $p = 0.077$. This test was run with nonequivalent groups however, six control, six free gallium, and only three GaDFO plates were tested. Tukey HSD post hoc analysis (Table

9) used to probe the interaction to see if any one factor acted as an outlier to skew the data but all interactions yielded a $p > 0.05$.

	Results		Comparison		
	Mean	SD	Trial A	Trial B	p value
Control	1.04E+11	1.04E+11	Control	Ga	0.121
Ga	1.83E+10	2.76E+10	Control	GaDFO	0.134
GaDFO	2.07E+09	2.08E+08	Ga	GaDFO	0.942
Control	4.40E+08	5.20E+07	Control	Amp	0.000
Amp	8.63E+06	9.84E+06	Control	Chlor	0.000
Chlor	2.37E+06	8.33E+05	Chlor	Amp	0.966

Table 9. *E. aerogenes* experiments resulted in no significant difference between the control experiments and the Ga and GaDFO trials.

Results from the *E. aerogenes* SPSS output as measured with control against antibiotic treatments indicated a significant effect between groups: control ($M = 4.4\text{x}10^8$, $SD = 5.2\text{x}10^7$), ampicillin ($M = 8.6\text{x}10^6$, $SD = 9.8\text{x}10^6$), and chloramphenicol ($M = 2.4\text{x}10^6$, $SD = 8.3\text{x}10^5$) F (2, 8) = 202.5, $p = 0.000$. The interaction was probed using the Tukey HSD post hoc analysis (Table 9) to determine which factors added to the significant difference between groups. Employing a 95% confidence interval, each measure of between groups testing was shown to be significant control*ampicillin $p = 0.000$, control*chloramphenicol $p = 0.000$, ampicillin*chloramphenicol $p = 0.966$.

HEK293 Mammalian Cell Culture

Culturing the HEK293 cells resulted in a slight decrease in cell number, as shown below:

Control	1.20×10^6 VC/mL
GaDFO	0.78×10^6 VC/mL
GaDFO with Penicillin/Streptomycin	0.89×10^6 VC/mL

Table 10. The culture of HEK293 cells led to a decrease in viable cells, both in the GaDFO enriched media, as well as the GaDFO enriched media with antibiotics. This could be caused by a variety of factors, and as such requires further study.

In addition, the growth of the cells in the DMEM media along with the GaDFO complex caused the media to slightly decrease its pH, as indicated by an orange tinge. The reported confluence of the GaDFO treated cells was roughly 75%, as compared to the control flask of HEK293 cells, which was 100% confluent.

Computational Analysis of DFO Biosynthesis and Siderophore Receptors

DFO Biosynthesis. Analysis of DesA amino acid sequences was expected to help explain why certain bacteria can uptake siderophores they do not synthesize. This analysis would therein support the hypothesis that many organisms will have the capacity to uptake our antimicrobial ligand. Phylogenetic analysis of the DesA amino acid yielded many organisms that met our criteria. The most common results included bacteria in the Actinobacteria class. Actinobacteria include such organisms but are not limited to *Streptomyces* spp., *Nocardiopsis* spp., and *Salinispora* spp. Other classes that appeared as positive hits included Alphaproteobacteria, Betaproteobacteria, Gammaproteobacteria, and Firmicutes. Table 11 contains a list of reported microbes with corresponding E values, and percent query coverage. The complete phylogenetic tree is presented in Figure 7.

Organism	Query Cover %	E value
Catenulispora acidiphila	97	0
Micromonospora lupini	98	0
Nonomuraea coxensis	98	0
Verrucosispora maris	97	0
Salinispora tropica	98	0
Salinispora arenicola	98	0
Nocardiopsis halotolerans	97	0
Nocardiopsis xinjiangensis	97	0
Nocardiopsis ganjiahuensis	98	0
Arthrobacter crystallopoietes	96	0
Pseudomonas luteola	98	0
Pseudomonas sp. HPB0071	98	0
Yersinia pestis	97	0
Methylobacter tundripaludum	98	0
Yersinia aldovae	97	0
Erwinia toletana	97	0
Bacillus megaterium	97	3.00E-112
Rhizobium giardinii	97	2.00E-107

Table 11. Select DesA homologues in nature. Table reports BLASTp results of DesA homologues. Criteria for reported hits included query coverage greater than 95%, and an E value less than 10^{-5}. Additionally, results were verified by ensuring the presence of desB, desC, and desD downstream of desA.

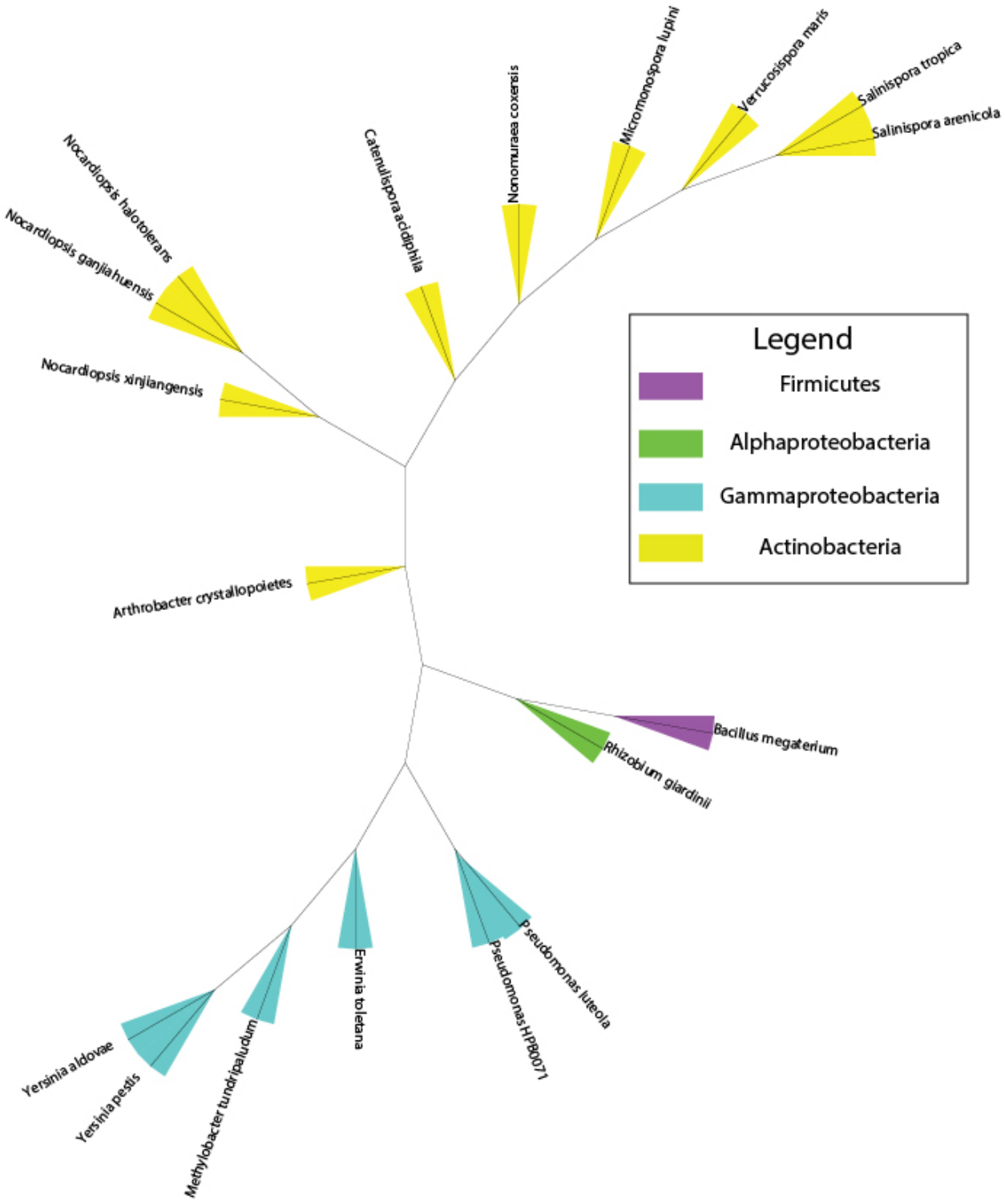

Figure 7. Examples of organisms with desferrioxamine biosynthesis genes. Proteins required for DFO biosynthesis include a PLP-dependent amino acid decarboxylase, an FAD-dependent amine monooxygense, an acyl CoA-dependent acyl transferase, and a protein with oligomerization and cyclization capabilities.. This phylogenetic tree was made using desA as the reference gene. BLAST was used to find homologous genes in other organisms, and Multiple Sequence Comparison by Log- Expectation (MUSCLE) software was used to compile the tree.

Siderophore Receptors. Receptor homology analysis yielded negative results as target organisms did not meet predetermined criteria. The closest organism to meet all standards was *A. faecalis* with an E value of $1x10^{-38}$, a query coverage of 98% and an AraC-like transcriptional regulator two genes upstream of the transporter. This receptor was annotated as a TonB-dependent siderophore receptor for ferric-coprogen and ferric-rhodotorulic acid (locus tag: G456DRAFT_03768). Interestingly, *A. faecalis* had eight genes that were annotated as TonB-dependent receptors as well.

Other target microbes included *E. aerogenes*, *E. coli*, and *S. aureus*. The most relevant *E. aerogenes* receptor was annotated as a ferrichrome iron receptor, a distinct siderophore. This transporter protein had an E value of $9x10^{-98}$, a query coverage of 92%, and an AraC-like transcriptional regulator two genes upstream of the transporter (similar to *A. faecalis*). Unlike *A. faecalis*, this bacterium only had five annotated siderophore receptors and they all had specific siderophores (e.g. ferrichrome or colicin).

The most relevant *E. coli* receptor was annotated as a TonB-dependent siderophore receptor for aerobactin. Certain pathogenic strains of *E. coli* synthesize aerobactin on their own (Neilands, 1995). This receptor had an E value of $3x10^{-108}$, a query coverage of 92%, but no AraC-like transcriptional regulator was found nearby. Although this bacterium had five TonB-dependent receptor genes, not all were associated with specific siderophores on the IMG database.

Finally, *S. aureus* had no significant hits since the query amino acid sequence came from *V. vulnificus*, a Gram-negative organism. Gram-positive bacteria like *S. aureus* cannot produce TonB-dependent receptors since they do not have outer

membranes. Thus, a known desferrioxamine receptor in Gram-positive bacteria could not be identified at this time.

Discussion

CAS Assay

The GaDFO CAS assay demonstrated the feasibility of synthesizing the GaDFO complex. DFO will successfully bind to free Ga ions at a one-to-one ratio and was shown to retain the Ga ions in the presence of other ligands (such as the CAS reagent). These findings can be seen in the Figure 4 (see results) and show that the moles of DFO pick up Ga ions as compared to the concentration of gallium bound to CAS. The feasibility of this system is very important as it means our project can move forward and begin using the GaDFO complex as a treatment possibility.

CFU & Microplate Analysis

A. faecalis. The total interaction of the one-way ANOVA yielded $F\,(2,8) = 72.619$, $p < 0.00$. This result indicates a statistically significant difference between the treatment conditions of the control, free gallium, and GaDFO. The use of the Tukey HSD post hoc analysis allowed for further understanding as to whether the results differed significantly enough to draw meaningful conclusions regarding the efficacy of treatment conditions. The Tukey HSD showed a $p = 0.003$ for the interaction between the free gallium and GaDFO conditions. This *p*-value indicates that there was a significant increase in treatment effectiveness as measured by the GaDFO than the free gallium treatments.

This result agrees with the microplate experiments, which show that GaDFO treatments were significantly different than the control in a range of $5.15x10^{-3}$ M to $5.15x10^{-6}$ M, and that GaDFO and Ga treatments were significantly different in a range of $5.15x10^{-3}$ M to $5.15x10^{-5}$ M.

E. coli. In addition to testing *E. coli* against a control, free gallium, and GaDFO condition, the bacteria were tested against ampicillin and chloramphenicol. The total interaction for testing on *E. coli* yielded F (4, 17) = 3.790, $p < 0.03$. Although this value is less significant than the total interaction shown by the ANOVA on *A. faecalis*, it is still below the parameters of a 5% margin of error, assuring that there was a statistically significant difference between conditions. Again, this interaction was probed by post hoc analysis. In post hoc analysis not all of the interactions were shown to be significantly different in their levels of CFU efficacy. There was a statistically significant difference between the control group and free gallium, $p = 0.002$ and the control group and GaDFO, $p = 0.000$. This interaction however was not found to be statistically significant when tested against the antibiotic treatments. In both the chloramphenicol and ampicillin outputs, the data was not found to be statistically different than the control. This could be explained by the a priori decision to use a 95% confidence interval, rather than an alpha of 0.1. This decision was made for convenience as it was consistent with the standard settings for one-way ANOVA analysis on SPSS. The observed values of $p = 0.070$ for chloramphenicol and $p = 0.066$ for ampicillin can, however, be argued to be statistically different enough from the control group to draw some, but minimal, conclusions. This relatively small difference between the antibiotic treatment groups and the control can

also potentially be explained by dilution of the antibiotics in treatment or human error in performing the CFU count.

Just as with the CFU experiments, the results of *E. coli* experiments in microplates are less clear than the *A. faecalis* results, but still useful; the GaDFO complex was statistically significantly different from the control for values of $5.15x10^{-3}$ and $5.15x10^{-4}$ M. It was also significantly different than the Ga only treatment at these levels.

E. aerogenes. Two separate trials were used to measure the efficacy of treatment types against *E. aerogenes*. The first trial tested the CFU count of a control against free gallium and GaDFO. This interaction did not yield statistically significant results, F (2, 14) = 3.191, p = 0.077. Although this interaction did not meet the alpha level cutoff of 0.05 chosen a priori, a significance level of $p < 0.1$ yields avenues for potential replication and strengthening of statistical findings. A potential factor could be the nonequivalent groups, six free gallium trials and only three GaDFO, or another aspect of systematic error. Because the DFO must successfully chelate the gallium in order for the GaDFO treatment to be effective, the relatively minimal difference seen may be explained by expired or contaminated DFO stocks that did not allow for the proper formation of the compound in solution. The post hoc analysis interactions have $p > 0.05$, suggesting unforeseen variation.

Results from the interaction of *E. aerogenes* against the antibiotics yielded a statistically significant difference between groups F (2, 8) = 202.479, p = 0.000. When probed in post hoc analysis, the interactions showed p = 0.000 between control and both types of antibiotics and each antibiotic was found to be relatively similar with a p = 0.966 interaction between ampicillin and chloramphenicol. This trial was used to give a relative

treatment difference between the efficacy of typical antibiotics against the free gallium and GaDFO treatments. However, relatively little can be discerned from the *E. aerogenes* analyses for two reasons: the tests were used against different biological replicates of the bacterium potentially affecting the reaction to treatments and nonequivalent groups used to test treatment differentials. Further testing must be done to elucidate reasons why *E. aerogenes* GaDFO treatments lacked statistical significance.

Microplate results match the CFU results for *E. aerogenes*. The GaDFO complex was only statistically significant from the control at the 5.15×10^{-3} M concentration (in which case it was also significantly different from the Ga only treatment).

Future Studies for CFU and Microplate Experiments. Future studies could aim to reproduce this work using a different, non-LB, iron-depleted media that would more accurately portray the environment in which bacteria naturally produce and acquire siderophores (Liermann et al., 2000), priming them to uptake more GaDFO. An iron-depleted environment is also clinically relevant because estimates claim that human bodies only have about 10^{-18} M of iron in free form (Kelson et al., 2013).

Another option for future research is to test GaDFO treatments on other bacteria. By further exploring which species are able to acquire this siderophore, treatment conditions could be further refined. This approach could also yield novel insights on siderophore transport systems and their specificity towards different siderophores. Areas of interest could include receptor specificity, chirality, backbone (i.e. the part of the siderophore structure that does not interact with iron), or the bacterial adaptation to iron-deplete conditions in the presence of a foreign siderophore (Miethke & Marahiel, 2007). Additionally, it would be beneficial to test the GaDFO treatment on BSL2 and BSL3

pathogens, which have a variety of iron-acquisition systems that could be exploited as potential targets for treatment methods of multidrug resistant bacteria (Kelson et al., 2013).

Eukaryotic Cell Culture

A final focus of our project was to take our treatment and see how it would affect mammalian cells. This was planned to be used as a cursory screen for future work, as it was done toward the end of the experimental phase of our research.

It has been shown that Ga^{3+} has no effect on the nicotinic acetylcholine receptors in human cells, as opposed to Al^{3+}, another trivalent cation (Hu, Li, Chen, & Li, 2007). This is relevant to the novel GaDFO treatment proposed in this paper in that this further supports the idea that the GaDFO is not likely to be harmful to mammalian cells *in vivo*. Furthermore, this research allows for future hypotheses regarding the treatments of GaDFO in animal models. It is important to note that this research only discusses nicotinic receptors. However, research regarding gallium interactions with other receptor types is needed to fully evaluate the toxic effects of gallium ions on mammalian cells.

HEK293 cells were used for the mammalian cell culture experiments. Padolska et al. (2012) showed that when plating HEK293 cells on AlGaN/GaN composites, the cells experienced what is considered a standard amount of growth. This implies that the gallium involved in the composite structure did not impede mammalian cell growth. This result is directly applicable to this study as it could provide support to our hypothesis that gallium bound with DFO might not harm mammalian cells in a significant way.

To further investigate this important question, future experimental work needs to be done. One of the most important issues is determining whether the cell line we used,

HEK293, is inherently resistant to the GaDFO complex. To prove this, the same experiments could be repeated using other common mammalian cell lines.

Computational Analysis of DFO Biosynthesis and Siderophore Receptors

A Note on Computer-Based Genomic Analysis. Computational analysis of genes and related encoded proteins has recently emerged as a powerful analytical tool. Decreased sequencing prices and increased computational power have contributed to widespread use of such technology (Richardson & Watson, 2013). However, most gene annotation software relies on fixed parameters predetermined by program developers, which may cause certain genes to go unnoticed. These parameters often tell programs to search for characteristics of a gene: a start codon sequence, a stop codon sequence, -35 bp and -10 bp consensus sequences upstream of the +1 transcription start site, or a Shine-Dalgarno sequence. Although these parameters are helpful for general search queries, excessively large/small genes, unique promoters, or start/stop codons may go unnoticed.

Annotation software uses sequence homology to associate gene products with known proteins and, as a result, genes that show enough similarity to a known protein will be assigned that label. This is perhaps one of the biggest pitfalls of genomic databases, as many genes are annotated incorrectly due to the large number of genomes that are currently being sequenced. As nearby genes or environmental factors may alter the functional properties of a protein, it is important to note that although a gene may be annotated with a specific name and share 100% similarity with a known protein, it does not mean that the gene product performs the same function as the known homologous protein. Computational data can be a powerful hypothesis-generating tool, but cannot be considered as definitive evidence without further proof (Richardson & Watson, 2013).

As stated previously, these experiments were performed to explore what organisms might be affected by the GaDFO treatment. Our approach to generate a hypothesis was two-fold. First, we searched for organisms that could synthesize desferrioxamine (in any of its forms), with the assumption that if an organism produces the siderophore, it should also have a receptor in place. Second, we examined siderophore receptors that shared significant homology with a known desferrioxamine B receptor from *Vibrio vulnificus* (the assumption here being that certain organisms may not produce siderophores, but may still rely on siderophore piracy).

DesA Homology. Phylogenetic analysis of DesA yielded a total of 18 organisms that matched desired criteria. Within these microbes, the most common representatives belonged to the phylum *Actinobacteria*. It is important to reiterate that this search excluded *Streptomyces* spp., as many microbes within this genus are known DFO-producers (Seipke, 2015).

Two interesting observations can be made from these results. First, the *Yersinia pestis* genome contains a region with strong homology to DesA (97% query coverage, and an E-value of 0.0; Locus tag: YPA_0823). Apart from this hypothetical *desA* gene, *Y. pestis* also has genes encoding for a putative monoxygenase, a putative acetyltransferase, and a fourth gene labeled as a "putative siderophore biosynthetic enzyme" directly downstream of the target gene (YPA_0823-0826). This organization is reminiscent to the one seen in *S. coelicolor*, and even has a number of putative siderophore transporter genes nearby (YPA_0827-0831). *Y. pestis* is the causative agent of the plague, and is currently of particular relevance due to bioterrorism applications (Zasada, Formińska, Zacharczuk, Jacob, & Grunow, 2015).

The presence of a homologous *desA* gene and potential siderophore receptors suggests that the GaDFO treatment could theoretically be absorbed by this microbe. This hypothesis is supported by data that shows that *Y. pestis* can utilize DFO-iron to grow at 26 °C (Lucier, Fetherston, Brubaker, & Perry, 1996). Interestingly, however, researchers found that the same does not hold true at 37 °C (generally considered to be body temperature).From our perspective, these findings are both discouraging and encouraging at the same time. On one hand, the fact that *Y. pestis* cannot utilize DFO at 37 °C suggests that GaDFO might not work as an oral, intramuscular, or intravenous antibiotic. However, a topical cream, or surface disinfectant, could still be a viable option (considering room temperature tends to be closer to 26 °C). An interesting short-term experiment would be to replicate Lucier et al.'s research (1996) with GaDFO, instead of DFO-iron.

Secondly, academic literature contains little evidence of *Y. pestis* producing DFO (or any similar derivatives). As a matter of fact, we were unable to find any articles that claim that *Y. pestis* produces siderophores other than Yersiniabactin (Ferreras, Ryu, Di Lello, Tan, & Quadri, 2005). This is interesting for two reasons. First, it is possible *Y. pestis* does not produce DFO because yersiniabactin is more efficient. If this is the case, it would be intriguing to create *Y. pestis* deletion mutants that are unable to produce yersiniabactin, to see if DFO production is upregulated. Second, it is possible DFO production is limited to very specific conditions (maybe never encountered by a common *Y. pestis* bacterium). This is feasible, considering that a similar phenomenon has been observed in *Streptomyces* spp. (Cao, Blodgett, & Clardy, 2010). If this is the case, future

experiments should address the conditions in which *Y. pestis* produces DFO, and how these conditions relate to the organism's lifestyle.

Siderophore Receptor. With regards to siderophore receptor analysis, most data yielded negative results. Possible explanations for this are the following. First, the homology search was aimed at the four organisms we used in CFU/microplate experiments. As a result, the sample size used to search for homologous proteins was considerably smaller. Second, criteria for positive results was rather strict. Specifically, the requirement of an AraC-like transcriptional activator directly upstream of a putative receptor may have limited our ability to find potential candidates. It is conceivable that AraC-like transcriptional regulators may be located further away from receptor genes. Overall, however, we have narrowed down a list of possible proteins responsible for GaDFO uptake in three of our four model organisms (*A. faecalis*, *E. aerogenes*, and *E. coli*). Future studies should focus on these proteins to evaluate specificity towards different siderophores.

Although receptor analysis for study model organisms yielded negative results, additional research was conducted on Gram-negative pathogens. Criteria used to search for hypothetical receptors remained the same. A list of evaluated pathogens is shown in Supplemental S2**.** Most organisms revealed no relevant hits. However, the enteric pathogen *Salmonella enterica* had encouraging homology.

Particularly, *S. enterica* serovars Typhimurium and Heidelberg both had homologues annotated as "ferrioxamine B receptors" according to BLASTp. The Heidelberg serovar had a query coverage of 97%, an E-value of $1x10^{-111}$, and an AraC-like receptor directly upstream of the hypothetical receptor gene. Typhimurium had a

query coverage of 93%, an E-value of $2x10^{-112}$, and an AraC-like receptor directly upstream of the hypothetical receptor gene as well. Both of these results provide other pathogens that could potentially uptake GaDFO. Upon further investigation, this hypothesis is consistent with findings that *S. enterica* serovar Typhimurium can uptake desferrioxamines B, E, and G (Kingsley et al., 1999). As such, *S. enterica* serovar Typhimurium could be a potential BSL-2 candidate to evaluate GaDFO efficiency.

Computational Analysis Summary. DFO biosynthesis/receptors yielded two possible future directions: evaluating GaDFO efficiency in *Y pestis,* and similarly in *S. enterica* serovar Typhimurium. These two organisms are known human pathogens and, as such, would be more meaningful targets to evaluate. If clinical relevance is considered, perhaps the more promising organism is *Y. pestis*. Although cases of *Y. pestis* infection in the United States are limited (CDC, 2013), the lack of an accepted plague vaccine, the potential threat of bioterrorism and the emergence of multidrug-resistant strains of this microbe (Feodorova & Motin, 2012) all highlight the importance of finding alternative treatments.

Conclusion

The goal of this study was to explore a new way of delivering metal ions to bacteria in an attempt to counter the growing number of antibiotic resistant bacterial strains. Desferrioxamine became the siderophore of choice due to its ability to form a complex with gallium in iron poor conditions, as indicated by the CAS assay, as well as its commercial availability. DFO's ability to deliver the toxic ion to the bacteria and

while not interacting with mammalian cells makes it a promising delivery system for treatments.

The CFU and microplate analyses demonstrate that the GaDFO complex has antibiotic potential. The data indicate that the GaDFO complex was more effective in inhibiting the growth of bacteria than the free gallium treatment condition. Testing mammalian cell growth in the presence of the GaDFO complex has shown that the complex may have potential for *in vivo* use. The GaDFO added to the media did not impede growth of HEK293 cells. This suggests that the GaDFO complex could be incorporated into traditional drug delivery systems to counteract antibiotic resistant bacterial infections. These results offer encouragement that this research can prove useful for the development of novel treatment types.

Future research can focus on testing different bacterial species, using different media, and using iron depleted media to further elucidate the antimicrobial properties of GaDFO complexes. Additionally, the results of this project could lead to the development of commercial products. One commercial application could be the development of topical solutions to prevent bacterial growth on different surfaces. Another commercial application could target undesired bacterial growth in algae farms that contribute to green energy.

As bacteria continue to develop resistance to currently available antibiotics, novel treatments must be developed to avoid a future where a simple bacterial infection can be deadly. This research lays the groundwork for a variety of applications, from human-use antibiotics to numerous industrial applications.

References

Aisenberg, G., Rolston, K. V., & Safdar, A. (2004). Bacteremia caused by *Achromobacter* and *Alcaligenes* species in 46 patients with cancer (1989–2003). *Cancer*, *101*(9), 2134–2140.

Alexander, J. W. (2009). History of the medical use of silver. *Surgical Infections*, *10*(3), 289–292.

Altschul, S. F., Gish, W., Miller, W., Myers, E. W., & Lipman, D. J. (1990). Basic local alignment search tool. *Journal of Molecular Biology*, *215*(3), 403–410.

Appelbaum, P. C. (2006). The emergence of vancomycin-intermediate and vancomycin-resistant *Staphylococcus aureus*. *Clinical Microbiology and Infection: The Official Publication of the European Society of Clinical Microbiology and Infectious Diseases*, *12 Suppl 1*, 16–23.

Autenrieth, I. B., Bohn, E., Ewald, J. H., & Heesemann, J. (1995). Deferoxamine B but not deferoxamine G1 inhibits cytokine production in murine bone marrow macrophages. *The Journal of Infectious Diseases*, *172*(2), 490–496.

Autenrieth, I. B., Reissbrodt, R., Saken, E., Berner, R., Vogel, U., Rabsch, W., & Heesemann, J. (1994). Desferrioxamine-promoted virulence of *Yersinia enterocolitica* in mice depends on both desferrioxamine type and mouse strain. *The Journal of Infectious Diseases*, *169*(3), 562–567.

Baba, T., Takeuchi, F., Kuroda, M., Yuzawa, H., Aoki, K., Oguchi, A., … Hiramatsu, K. (2002). Genome and virulence determinants of high virulence community-acquired MRSA. *Lancet*, *359*(9320), 1819–1827.

Barbosa, T. M., & Levy, S. B. (2000). The impact of antibiotic use on resistance development and persistence. *Drug Resistance Updates: Reviews and Commentaries in Antimicrobial and Anticancer Chemotherapy*, *3*(5), 303–311.

Barona-Gómez, F., Lautru, S., Francou, F.-X., Leblond, P., Pernodet, J.-L., & Challis, G. L. (2006). Multiple biosynthetic and uptake systems mediate siderophore-dependent iron acquisition in *Streptomyces coelicolor* A3(2) and Streptomyces ambofaciens ATCC 23877. *Microbiology (Reading, England)*, *152*(Pt 11), 3355–3366.

Barona-Gómez, F., Wong, U., Giannakopulos, A. E., Derrick, P. J., & Challis, G. L. (2004). Identification of a cluster of genes that directs desferrioxamine biosynthesis in *Streptomyces coelicolor* M145. *Journal of the American Chemical Society*, *126*(50), 16282–16283.

Barrett, T. A., Wu, A., Zhang, H., Levy, M. S., & Lye, G. J. (2010). Microwell engineering characterization for mammalian cell culture process development. *Biotechnology and Bioengineering*, *105*(2), 260–275.

Bauer, T. M., Ofner, E., Just, H. M., Just, H., & Daschner, F. D. (1990). An epidemiological study assessing the relative importance of airborne and direct contact transmission of microorganisms in a medical intensive care unit. *The Journal of Hospital Infection*, *15*(4), 301–309.

Beasley, F. C., & Heinrichs, D. E. (2010). Siderophore-mediated iron acquisition in the staphylococci. *Journal of Inorganic Biochemistry*, *104*(3), 282–288.

Beasley, F. C., Marolda, C. L., Cheung, J., Buac, S., & Heinrichs, D. E. (2011). *Staphylococcus aureus* transporters Hts, Sir, and Sst capture iron liberated from human transferrin by Staphyloferrin A, Staphyloferrin B, and catecholamine stress hormones, respectively, and contribute to virulence. *Infection and Immunity*, *79*(6), 2345–2355.

Bentley, S. D., Chater, K. F., Cerdeño-Tárraga, A.-M., Challis, G. L., Thomson, N. R., James, K. D., … Hopwood, D. A. (2002). Complete genome sequence of the model actinomycete *Streptomyces coelicolor* A3(2). *Nature*, *417*(6885), 141–147.

Benveniste, R., & Davies, J. (1973). Mechanisms of Antibiotic Resistance in Bacteria. *Annual Review of Biochemistry*, *42*(1), 471–506.

Bernstein, L. R. (1998). Mechanisms of Therapeutic Activity for Gallium. *Pharmacological Reviews*, *50*(4), 665–682.

Braydich-Stolle, L., Hussain, S., Schlager, J. J., & Hofmann, M.-C. (2005). In Vitro Cytotoxicity of Nanoparticles in Mammalian Germline Stem Cells. *Toxicological Sciences : An Official Journal of the Society of Toxicology*, *88*(2), 412–419.

Cao, S., Blodgett, J. A. V., & Clardy, J. (2010). Targeted Discovery of Polycyclic Tetramate Macrolactams from an Environmental *Streptomyces* Strain. *Organic Letters*, *12*(20), 4652–4654.

Centers for Disease Control and Prevention (2004) Inpatient Surgery. Retrieved from http://www.cdc.gov/nchs/fastats/inpatient-surgery.htm

Centers for Disease Control and Prevention. (2009) CAUTI Guideline - HICPAC. Retrieved from http://www.cdc.gov/hicpac/cauti/001_cauti.html

Centers for Disease Control and Prevention. (2013) Heart Disease Facts and Statistics. Retrieved from http://www.cdc.gov/heartdisease/statistics.htm

Challis, G. L. (2005). A widely distributed bacterial pathway for siderophore biosynthesis independent of nonribosomal peptide synthetases. *Chembiochem: A European Journal of Chemical Biology*, *6*(4), 601–611.

Chaturvedi, K., Sun, S. Y., O'Brien, T., Liu, Y. J., & Brooks, J. W. (2014). Comparison of the behavior of CHO cells during cultivation in 24-square deep well microplates and conventional shake flask systems. *Biotechnology Reports*, *1–2*, 22–26.

Chen, L. F., Arduino, J. M., Sheng, S., Muhlbaier, L. H., Kanafani, Z. A., Harris, A. D., … Fowler Jr, V. G. (2012). Epidemiology and outcome of major postoperative infections following cardiac surgery: Risk factors and impact of pathogen type. *American Journal of Infection Control*, *40*(10), 963–968.

Chitambar, C. R. (2010). Medical Applications and Toxicities of Gallium Compounds. *International Journal of Environmental Research and Public Health*, *7*(5), 2337–2361.

Chopra, I., & Roberts, M. (2001). Tetracycline antibiotics: mode of action, applications, molecular biology, and epidemiology of bacterial resistance. *Microbiology and Molecular Biology Reviews: MMBR*, *65*(2), 232–260 ; second page, table of contents.

Cohen, M. L. (2000). Changing patterns of infectious disease. *Nature*, *406*(6797), 762–767.

Crosa, J. H., & Walsh, C. T. (2002). Genetics and assembly line enzymology of siderophore biosynthesis in bacteria. *Microbiology and Molecular Biology Reviews: MMBR*, *66*(2), 223–249.

Dale, S. E., Doherty-Kirby, A., Lajoie, G., & Heinrichs, D. E. (2004). Role of siderophore biosynthesis in virulence of *Staphylococcus aureus*: identification and characterization of genes involved in production of a siderophore. *Infection and Immunity*, *72*(1), 29–37.

Delcour, A. H. (2009). Outer membrane permeability and antibiotic resistance. *Biochimica et Biophysica Acta (BBA) - Proteins and Proteomics*, *1794*(5), 808–816.

Dini, C., & Aszodi, J. (2000). Synthesis of a dihydroxythiophene analogue of catechosporines. *Bioorganic & Medicinal Chemistry Letters*, *10*(4), 349–352.

Dizaj, S. M., Lotfipour, F., Barzegar-Jalali, M., Zarrintan, M. H., & Adibkia, K. (2014). Antimicrobial activity of the metals and metal oxide nanoparticles. *Materials Science and Engineering: C*, *44*, 278–284.

Doebbeling, B. N., Stanley, G. L., Sheetz, C. T., Pfaller, M. A., Houston, A. K., Annis, L., … Wenzel, R. P. (1992). Comparative efficacy of alternative hand-washing agents in reducing nosocomial infections in intensive care units. *The New England Journal of Medicine*, *327*(2), 88–93.

Edgar, R. C. (2004). MUSCLE: multiple sequence alignment with high accuracy and high throughput. *Nucleic Acids Research*, *32*(5), 1792–1797.

Feodorova, V. A., & Motin, V. L. (2012). Plague vaccines: current developments and future perspectives. *Emerging Microbes & Infections*, *1*(11), e36.

Ferreras, J. A., Ryu, J.-S., Di Lello, F., Tan, D. S., & Quadri, L. E. N. (2005). Small-molecule inhibition of siderophore biosynthesis in *Mycobacterium tuberculosis* and *Yersinia pestis*. *Nature Chemical Biology*, *1*(1), 29–32.

Flo, T. H., Smith, K. D., Sato, S., Rodriguez, D. J., Holmes, M. A., Strong, R. K., … Aderem, A. (2004). Lipocalin 2 mediates an innate immune response to bacterial infection by sequestrating iron. *Nature*, *432*(7019), 917–921.

Fluckinger, M., Haas, H., Merschak, P., Glasgow, B. J., & Redl, B. (2004). Human Tear Lipocalin Exhibits Antimicrobial Activity by Scavenging Microbial Siderophores. *Antimicrobial Agents and Chemotherapy*, *48*(9), 3367–3372.

Freeman, V. J., & Morse, I. U. (1952). Further Observations on the Change to Virulence of Bacteriophage-Infected Avirulent Strains of *Corynebacterium Diphtheriae*. *Journal of Bacteriology*, *63*(3), 407–414.

Gaynes, R. P., Edwards, J. R., Jarvis, W. R., Culver, D. H., Tolson, J. S., & Martone, W. J. (1996). Nosocomial Infections Among Neonates in High-risk Nurseries in the United States. *Pediatrics*, *98*(3), 357–361.

Goetz, D. H., Holmes, M. A., Borregaard, N., Bluhm, M. E., Raymond, K. N., & Strong, R. K. (2002). The neutrophil lipocalin NGAL is a bacteriostatic agent that interferes with siderophore-mediated iron acquisition. *Molecular Cell*, *10*(5), 1033–1043.

Górska, A., Sloderbach, A., & Marszałł, M. P. (2014). Siderophore-drug complexes: potential medicinal applications of the "Trojan horse" strategy. *Trends in Pharmacological Sciences*, *35*(9), 442–449.

Hall, B. G., Acar, H., Nandipati, A., & Barlow, M. (2014). Growth rates made easy. *Molecular Biology and Evolution*, *31*(1), 232–238.

Han, S., Zaniewski, R. P., Marr, E. S., Lacey, B. M., Tomaras, A. P., Evdokimov, A., … Shanmugasundaram, V. (2010). Structural basis for effectiveness of siderophore-conjugated monocarbams against clinically relevant strains of *Pseudomonas aeruginosa*. *Proceedings of the National Academy of Sciences of the United States of America*, *107*(51), 22002–22007.

Hantke, K. (2001). Iron and metal regulation in bacteria. *Current Opinion in Microbiology*, *4*(2), 172–177.

Harris, W. R. (1983). Thermodynamic binding constants of the zinc-human serum transferrin complex. *Biochemistry*, *22*(16), 3920–3926.

Hartmann, A., Fiedler, H. P., & Braun, V. (1979). Uptake and conversion of the antibiotic albomycin by *Escherichia coli* K-12. *European Journal of Biochemistry / FEBS*, *99*(3), 517–524.

Hartwig, A. (1995). Current aspects in metal genotoxicity. *Biometals*, *8*(1), 3–11.

Holzman, R. S., Florman, A. L., & Lyman, M. (1980). Gentamicin resistant and sensitive strains of *S. aureus*. Factors affecting colonization and virulence for infants in a special care nursery. *American Journal of Epidemiology*, *112*(3), 352–361.

Hoyer, O. (2012, February 20). Optimization of mixing parameters in lab automation. [Web log comment]. Retrieved from http://www.thermoshaker.com/?tag=orbital- shaker

Huson, D. H., & Scornavacca, C. (2012). Dendroscope 3: An Interactive Tool for Rooted Phylogenetic Trees and Networks. *Systematic Biology*, sys062.

Hu, X., & Boyer, G. L. (1996). Siderophore-Mediated Aluminum Uptake by *Bacillus megaterium* ATCC 19213. *Applied and Environmental Microbiology*, *62*(11), 4044–4048.

Hu, W.-P., Li, X.-M., Chen, J.-G., & Li, Z.-W. (2007). Potentiation of the nicotinic acetylcholine receptor by aluminum in mammalian neurons. *Neuroscience*, *149*(1), 1–6.

Jagobs, J., Greene, H., & Gendel, B. R. (1965). Acute Iron Intoxication. *New England Journal of Medicine*, *273*(21), 1124–1127.

Jiang, L., Garrick, M. D., Garrick, L. M., Zhao, L., & Collins, J. F. (2013). Divalent metal transporter 1 (Dmt1) mediates copper transport in the duodenum of iron-deficient rats and when overexpressed in iron-deprived HEK-293 cells. *The Journal of Nutrition*, *143*(12), 1927–1933.

Ji, C., Miller, P. A., & Miller, M. J. (2012). Iron Transport-Mediated Drug Delivery: Practical Syntheses and In Vitro Antibacterial Studies of Tris-catecholate Siderophore-Aminopenicillin Conjugates Reveals Selectively Potent Anti-Pseudomonal Activity. *Journal of the American Chemical Society*, *134*(24), 9898–9901.

Kaneko, Y., Thoendel, M., Olakanmi, O., Britigan, B. E., & Singh, P. K. (2007). The transition metal gallium disrupts *Pseudomonas aeruginosa* iron metabolism and has antimicrobial and antibiofilm activity. *The Journal of Clinical Investigation*, *117*(4), 877–888.

Kehrer, J. P. (2000). The Haber-Weiss reaction and mechanisms of toxicity. *Toxicology*, *149*(1), 43–50.

Kelson, A. B., Carnevali, M., & Truong-Le, V. (2013). Gallium-based anti-infectives: targeting microbial iron-uptake mechanisms. *Current Opinion in Pharmacology*, *13*(5), 707–716.

Kingsley, R. A., Reissbrodt, R., Rabsch, W., Ketley, J. M., Tsolis, R. M., Everest, P., … Williams, P. H. (1999). Ferrioxamine-Mediated Iron(III) Utilization by

Salmonella enterica. *Applied and Environmental Microbiology*, *65*(4), 1610–1618.

Kohanski, M. A., Dwyer, D. J., & Collins, J. J. (2010). How antibiotics kill bacteria: from targets to networks. *Nature Reviews. Microbiology*, *8*(6), 423–435.

Kollef, M. H., Sharpless, L., Vlasnik, J., Pasque, C., Murphy, D., & Fraser, V. J. (1997). THe impact of nosocomial infections on patient outcomes following cardiac surgery. *Chest*, *112*(3), 666–675.

Langmyhr, F. J., & Klausen, K. S. (1963). Complex formation of iron (III) with Chrome Azurol S. *Analytica Chimica Acta*, *29*, 149–167.

Lara, H. H., Ayala-Núñez, N. V., Turrent, L. del C. I., & Padilla, C. R. (2009). Bactericidal effect of silver nanoparticles against multidrug-resistant bacteria. *World Journal of Microbiology and Biotechnology*, *26*(4), 615–621.

Lau, C. Y., Zahidi, A. A. A., Liew, O. W., & Ng, T. W. (2015). A direct heating model to overcome the edge effect in microplates. *Journal of Pharmaceutical and Biomedical Analysis*, *102*, 199–202.

Lemire, J. A., Harrison, J. J., & Turner, R. J. (2013). Antimicrobial activity of metals: mechanisms, molecular targets and applications. *Nature Reviews Microbiology*, *11*(6), 371–384.

Letunic, I., & Bork, P. (2011). Interactive Tree Of Life v2: online annotation and display of phylogenetic trees made easy. *Nucleic Acids Research*, *39*(Web Server issue), W475–478.

Levy, S. B. (1982). Microbial resistance to antibiotics. An evolving and persistent problem. *Lancet*, *2*(8289), 83–88.

Levy, S. B., & Marshall, B. (2004). Antibacterial resistance worldwide: causes, challenges and responses. *Nature Medicine*, *10*(12 Suppl), S122–129.

Liermann, L. J., Kalinowski, B. E., Brantley, S. L., & Ferry, J. G. (2000). Role of bacterial siderophores in dissolution of hornblende. *Geochimica et Cosmochimica Acta*, *64*(4), 587–602.

Ling, L. L., Schneider, T., Peoples, A. J., Spoering, A. L., Engels, I., Conlon, B. P., … Lewis, K. (2015). A new antibiotic kills pathogens without detectable resistance. *Nature*, *517*(7535), 455–459.

Lucier, T. S., Fetherston, J. D., Brubaker, R. R., & Perry, R. D. (1996). Iron uptake and iron-repressible polypeptides in *Yersinia pestis*. *Infection and Immunity*, *64*(8), 3023–3031.

Markowitz, V. M., Chen, I.-M. A., Palaniappan, K., Chu, K., Szeto, E., Grechkin, Y., … Kyrpides, N. C. (2012). IMG: the integrated microbial genomes database and comparative analysis system. *Nucleic Acids Research*, *40*(D1), D115–D122.

Martinez, J. L., & Baquero, F. (2000). Mutation Frequencies and Antibiotic Resistance. *Antimicrobial Agents and Chemotherapy*, *44*(7), 1771–1777.

Matejcek, A., & Goldman, R. D. (2013). Treatment and prevention of ophthalmia neonatorum. *Canadian Family Physician*, *59*(11), 1187–1190.

Menninger, J. R., & Otto, D. P. (1982). Erythromycin, carbomycin, and spiramycin inhibit protein synthesis by stimulating the dissociation of peptidyl-tRNA from ribosomes. *Antimicrobial Agents and Chemotherapy*, *21*(5), 811–818.

Miethke, M., & Marahiel, M. A. (2007). Siderophore-based iron acquisition and pathogen control. *Microbiology and Molecular Biology Reviews: MMBR*, *71*(3), 413–451.

Miller, M. J., McKee, J. A., Minnick, A. A., & Dolence, E. K. (1991). The design, synthesis and study of siderophore-antibiotic conjugates. Siderophore mediated drug transport. *Biology of Metals*, *4*(1), 62–69.

Moeck, G. S., & Coulton, J. W. (1998). TonB-dependent iron acquisition: mechanisms of siderophore-mediated active transport. *Molecular Microbiology*, *28*(4), 675–681.

Mole, B. (2013). MRSA: Farming up trouble. *Nature*, *499*(7459), 398–400.

Morin, N., Lanneluc, I., Connil, N., Cottenceau, M., Pons, A. M., & Sablé, S. (2011). Mechanism of Bactericidal Activity of Microcin L in *Escherichia coli* and Salmonella enterica. *Antimicrobial Agents and Chemotherapy*, *55*(3), 997–1007.

Morones, J. R., Elechiguerra, J. L., Camacho, A., Holt, K., Kouri, J. B., Ramírez, J. T., & Yacaman, M. J. (2005). The bactericidal effect of silver nanoparticles. *Nanotechnology*, *16*(10), 2346. http://doi.org/10.1088/0957-4484/16/10/059

Murray, P. R., Rosenthal, K. S., & Pfaller, M. A. (2009). *Medical microbiology*. Philadelphia: Mosby/Elsevier.

Mushtaq, S., Warner, M., & Livermore, D. (2010). Activity of the siderophore monobactam BAL30072 against multiresistant non-fermenters. *The Journal of Antimicrobial Chemotherapy*, *65*(2), 266–270.

Neilands, J. B. (1995). Siderophores: Structure and Function of Microbial Iron Transport Compounds. *Journal of Biological Chemistry*, *270*(45), 26723–26726.

Neu, H. C. (1992). The Crisis in Antibiotic Resistance. *Science*, *257*(5073), 1064–1073.

Nikaido, H. (2003). Molecular basis of bacterial outer membrane permeability revisited. *Microbiology and Molecular Biology Reviews: MMBR*, *67*(4), 593–656.

Nikaido, H., & Rosenberg, E. Y. (1990). Cir and Fiu proteins in the outer membrane of *Escherichia coli* catalyze transport of monomeric catechols: study with beta-lactam antibiotics containing catechol and analogous groups. *Journal of Bacteriology*, *172*(3), 1361–1367.

Page, M. G. P., Dantier, C., & Desarbre, E. (2010). In Vitro Properties of BAL30072, a Novel Siderophore Sulfactam with Activity against Multiresistant Gram-Negative Bacilli. *Antimicrobial Agents and Chemotherapy*, *54*(6), 2291–2302.

Perry, R. D., & Brubaker, R. R. (1979). Accumulation of iron by *Yersiniae*. *Journal of Bacteriology*, *137*(3), 1290–1298.

Pierce, G. E. (2005). *Pseudomonas aeruginosa, Candida albicans,* and device-related nosocomial infections: implications, trends, and potential approaches for control. *Journal of Industrial Microbiology and Biotechnology*, *32*(7), 309–318.

Podolska, A., Tham, S., Hart, R. D., Seeber, R. M., Kocan, M., Kocan, M., & ... Nener, B. D. (2012). Biocompatibility of semiconducting AlGaN/GaN material with living cells. *Sensors & Actuators B: Chemical*, *169*401-406.

Rabsch, W., Voigt, W., Reissbrodt, R., Tsolis, R. M., & Bäumler, A. J. (1999). *Salmonella typhimurium* IroN and FepA proteins mediate uptake of *Enterobactin* but differ in their specificity for other siderophores. *Journal of Bacteriology*, *181*(11), 3610–3612.

Rai, M., Yadav, A., & Gade, A. (2009). Silver nanoparticles as a new generation of antimicrobials. *Biotechnology Advances*, *27*(1), 76–83.

Rappé, M. S., & Giovannoni, S. J. (2003). The uncultured microbial majority. *Annual Review of Microbiology*, *57*, 369–394.

Raymond, K. N., Müller, G., & Matzanke, B. F. (1984). Complexation of iron by siderophores a review of their solution and structural chemistry and biological function. In *Structural Chemistry* (pp. 49–102). Springer Berlin Heidelberg.

Reniere, M., Pishcany, G., Skaar, E. (2010). Iron Uptake in *Staphylococci: Iron Uptake and Homeostasis in Microorganisms*. Horizon Scientific Press.

Richards, M. J., Edwards, J. R., Culver, D. H., & Gaynes, R. P. (1999). Nosocomial Infections in Pediatric Intensive Care Units in the United States. *Pediatrics*, *103*(4), e39–e39.

Richardson, E. J., & Watson, M. (2013). The automatic annotation of bacterial genomes. *Briefings in Bioinformatics*, *14*(1), 1–12.

Russell, A. D., & Hugo, W. B. (1994). Antimicrobial activity and action of silver. *Progress in Medicinal Chemistry*, *31*, 351–370.

Sayyed, S. B. C. (2006). Purification of siderophores of *Alcaligenes faecalis* on Amberlite XAD. *Bioresource Technology*, *97*(8), 1026–9.

Sanders, W. E., & Sanders, C. C. (1997). *Enterobacter spp*.: pathogens poised to flourish at the turn of the century. *Clinical Microbiology Reviews*, *10*(2), 220–241.

Schubert, S., & Autenrieth, I. B. (2000). Conjugation of hydroxyethyl starch to desferrioxamine (DFO) modulates the dual role of DFO in *Yersinia enterocolitica* infection. *Clinical and Diagnostic Laboratory Immunology*, *7*(3), 457–462.

Schwyn, B., & Neilands, J. B. (1987). Universal chemical assay for the detection and determination of siderophores. *Analytical Biochemistry*, *160*(1), 47–56.

Seipke, R. F. (2015). Strain-Level Diversity of Secondary Metabolism in *Streptomyces albus*. *PLOS ONE*, *10*(1), e0116457.

Sims, J. M. (1884). *The Story of My Life*. D. Appleton.

Spellberg, B., Guidos, R., Gilbert, D., Bradley, J., Boucher, H. W., Scheld, W. M., … Infectious Diseases Society of America. (2008). The epidemic of antibiotic-resistant infections: a call to action for the medical community from the Infectious Diseases Society of America. *Clinical Infectious Diseases: An Official Publication of the Infectious Diseases Society of America*, *46*(2), 155–164.

Tanabe, T., Takata, N., Naka, A., Moon, Y.-H., Nakao, H., Inoue, Y., … Yamamoto, S. (2005). Identification of an AraC-like regulator gene required for induction of the 78-kDa ferrioxamine B receptor in *Vibrio vulnificus*. *FEMS Microbiology Letters*, *249*(2), 309–314.

Tanner, A. (n.d.). Helpful Hints to Manage Edge Effect of Cultured Cells for High Throughput Screening.

Tenover, F. C., Weigel, L. M., Appelbaum, P. C., McDougal, L. K., Chaitram, J., McAllister, S., … Bozdogan, B. (2004). Vancomycin-resistant *Staphylococcus aureus* isolate from a patient in Pennsylvania. *Antimicrobial Agents and Chemotherapy*, *48*(1), 275–280.

Traxler, M. F., Seyedsayamdost, M. R., Clardy, J., & Kolter, R. (2012). Interspecies modulation of bacterial development through iron competition and siderophore piracy. *Molecular Microbiology*, *86*(3), 628–644.

Van Bambeke, F., Balzi, E., & Tulkens, P. M. (2000). Antibiotic efflux pumps. *Biochemical Pharmacology*, *60*(4), 457–470.

Vargaftik, N. B., Volkov, B. N., & Voljak, L. D. (1983). International Tables of the Surface Tension of Water. *Journal of Physical and Chemical Reference Data*, *12*(3), 817–820.

Vassiliadis, G., Destoumieux-Garzón, D., Lombard, C., Rebuffat, S., & Peduzzi, J. (2010). Isolation and Characterization of Two Members of the Siderophore-Microcin Family, Microcins M and H47. *Antimicrobial Agents and Chemotherapy*, *54*(1), 288–297.

Vértesy, L., Aretz, W., Fehlhaber, H.-W., & Kogler, H. (1995). Salmycin A–D, Antibiotika aus Streptomyces violaceus, DSM 8286, mit Siderophor-Aminoglycosid-Struktur. *Helvetica Chimica Acta*, *78*(1), 46–60.

Walsh, C. (2000). Molecular mechanisms that confer antibacterial drug resistance. *Nature*, *406*(6797), 775–781.

Wardman, P., & Candeias, L. P. (1996). Fenton Chemistry: An Introduction. *Radiation Research*, *145*(5), 523–531.

WHO | Antimicrobial resistance: global report on surveillance. (2014). Retrieved from http://www.who.int/drugresistance/documents/surveillancereport/

Wilke, M. S., Lovering, A. L., & Strynadka, N. C. J. (2005). Beta-lactam antibiotic resistance: a current structural perspective. *Current Opinion in Microbiology*, *8*(5), 525–533.

Wong, G. B., Kappel, M. J., Raymond, K. N., Matzanke, B., & Winkelmann, G. (1983). Coordination chemistry of microbial iron transport compounds. 24. Characterization of coprogen and ferricrocin, two ferric hydroxamate siderophores. *Journal of the American Chemical Society*, *105*(4), 810–815.

Woodard, B., Knapstein, K., Barrett, J. (2013). *Fermentation Science and Biopharmaceutical Production*. Deale, MD: Vandalay Publishing.

Yamanaka, K., Oikawa, H., Ogawa, H., Hosono, K., Shinmachi, F., Takano, H., … Ueda, K. (2005). Desferrioxamine E produced by *Streptomyces griseus* stimulates

growth and development of *Streptomyces tanashiensis*. *Microbiology (Reading, England)*, *151*(Pt 9), 2899–2905.

Zasada, A. A., Formińska, K., Zacharczuk, K., Jacob, D., & Grunow, R. (2015). Comparison of eleven commercially available rapid tests for detection of *Bacillus anthracis* , *Francisella tularensis* and *Yersinia pestis*. *Letters in Applied Microbiology*, n/a–n/a.

Zimmermann, H. F., John, G. T., Trauthwein, H., Dingerdissen, U., & Huthmacher, K. (2003). Rapid evaluation of oxygen and water permeation through microplate sealing tapes. *Biotechnology Progress*, *19*(3), 1061–1063.

Zurenko, G. E., Truesdell, S. E., Yagi, B. H., Mourey, R. J., & Laborde, A. L. (1990). In vitro antibacterial activity and interactions with beta-lactamases and penicillin-binding proteins of the new monocarbam antibiotic U-78608. *Antimicrobial Agents and Chemotherapy*, *34*(5), 884–888.

Appendix A: Protocols

A1: Microplate Fermentation Protocol

Materials:

0.17156 M Gallium stock solution (single 50 mL conical is sufficient)

DFO mesylate salt, solid

sixteen 50 mL conical tubes

eight 50 mL conical filters.

2.2x LB

Early log-phase culture of all bacteria to be tested

Stock preparation

1. Weigh out 0.752 g of DFO mesylate and add to 50 mL of autoclaved DI water. This is the 2.29×10^{-2} M DFO stock, "DFO 2"
2. Add 6mL of gallium stock solution to 44mL autoclaved DI water. This is the 2.06×10^{-2} M Ga stock, "Ga 2"
3. Prepare stocks 3, 4 and 5 of Ga and DFO as follows:

DFO 3: 5 mL DFO 2 45.000 mL autoclaved DI water	DFO 4: 0.500 mL DFO 2 49.500 mL autoclaved DI water	DFO 5: 0.050 mL DFO 2 49.950 mL autoclaved DI water
Ga 3: 5 mL Ga 2 45.000 mL autoclaved DI water	Ga 4: 0.500 mL Ga 2 49.500 mL autoclaved DI water	Ga 5: 0.050 mL Ga 2 49.950 mL autoclaved DI water

Using these stocks and the 2.2x LB, prepare stocks A-H as follows:

Stock A: 10 mL DFO 2 10 mL Ga 2	Stock B: 10 mL DFO 3 10 mL Ga 3	Stock C: 10 mL DFO 4 10 mL Ga 4	Stock D: 10 mL DFO 5 10 mL Ga 5

18 mL 2.2x LB	18 mL 2.2x LB	18 mL 2.2x LB	18 mL 2.2xLB
Stock E: 10 mL autoclaved DI water 10 mL Ga 2 18 mL 2.2xLB	Stock F: 10 mL autoclaved DI water 10 mL Ga 3 18 mL 2.2x LB	Stock G: 10 mL autoclaved DI water 10 mL Ga 4 18 mL 2.2x LB	Stock H: 10 mL autoclaved DI water 10 mL Ga 5 18 mL 2.2x LB

Microplate Setup

1. Measure the OD of the log phase culture and dilute to an OD of 0.3
2. Setup plate as desired, using 1-2 mL of each stock per well. See 3 for planning purposes.
3. Add 0.050 mL of OD 0.3 culture for every 0.950 mL of stock in each well. It is easiest to use either 0.950 mL or 1.9 mL.
4. Activate the microplate reader
5. Go “Wizard” and click OK repeatedly until all boxes disappear.
6. Click “New”
7. Click “Settings”
8. Select Falcon 24 Well (or other appropriate plate), 37 °C with temperature control activated, shaking intensity 3, and desired duration and sampling frequency under kinetic parameters
9. Make sure the reader is set to “absorbance” and 600 nm
10. Click “OK” in the settings box
11. Click “Read” and follow the instructions.

A2: CAS protocol:

This protocol is adapted from Schwyn and Neilands (1987) and scaled up and modified for convenience. Addition of iron is omitted because this CAS solution is intended to detect gallium. Since gallium concentrations will be variable, no gallium is added to the stock solution.

Materials:

1 L volumetric flask

Chrome Azurol S 50% (Aldrich 199532)

Hexadecyltrimethylammonium bromide (HDTMA) (Sigma H6269)

Piperazine (make unknown)

Hydrochloric Acid, concentrated (make unknown)

CAS Reagent Preparation:

1. Rinse volumetric flask with 6 M HCl
2. Rinse volumetric flask with DI water 3 times
3. Dissolve 43.07 g piperazine in DI water in volumetric flask
4. Add 62.5 mL concentrated HCl to flask
5. Add 0.18 g CAS to flask
6. Add 0.218 g HDTMA to flask
7. Parafilm top of flask and carefully invert until all phases mix and bubbling subsides. Bleed air from top of flask if parafilm is bulging outward.
8. Filter resulting solution (0.22 micron is sufficient, non-sterile paper filters work as well)
9. Store filtered solution in opaque plastic bottle in a cool area
10. Note solution OD590 after filtering (take 5 samples)

11. Before each use, compare 5 samples to original OD590 to confirm that solution is not degrading

The CAS reagent has the following properties:

[CAS] = 0.149 mM (this number is approximate, some CAS may be removed in the filtering process)

[HDTMA] = 0.598 mM

[Piperazine] = 500 mM

pH = ~5.6 (half equivalence point, depends on exact acid concentration)

Plate Preparations:

GaCAS plate preparation

Have on hand:

0.05 mM $GaCl_3$ stock

CAS reagent mix

Two 24 well plates (Falcon)

Prepare plate as follows:

All wells: 1000 µL CAS reagent mix

1000 µL Ga stock 25 µM Ga	900 µL Ga stock 100 µL DI water 22.5 µM Ga	800 µL Ga stock 200 µL Water 20 µM Ga	700 µL Ga stock 300 µL DI water 17.5 µM Ga	600 µL Ga stock 400 µL DI water 15 µM Ga	
1000 µL Ga stock 25 µM Ga	900 µL Ga stock 100 µL DI water	800 µL Ga stock 200 µL Water 20 µM Ga	700 µL Ga stock 300 µL DI water	600 µL Ga stock 400 µL DI water 15 µM Ga	

	22.5 µM Ga		17.5 µM Ga		
1000 µL Ga stock 25 µM Ga	900 µL Ga stock 100 µL DI water 22.5 µM Ga	800 µL Ga stock 200 µL Water 20 µM Ga	700 µL Ga stock 300 µL DI water 17.5 µM Ga	600 µL Ga stock 400 µL DI water 15 µM Ga	
1000µL Ga stock 25µM Ga	900 µL Ga stock 100 µL DI water 22.5 µM Ga	800 µL Ga stock 200 µL Water 20 µM Ga	700 µL Ga stock 300 µL DI water 17.5 µM Ga	600 µL Ga stock 400 µL DI water 15 µM Ga	

500 µL Ga stock 500 µL DI water 12.5 µM Ga	400 µL Ga stock 600 µL DI water 10 µM Ga	300 µL Ga stock 700 µL DI water 7.5 µM Ga	200 µL Ga stock 800 µL DI water 5 µM Ga	100 µL Ga stock 900 µL water 2.5 µM Ga	1000 µL DI water 0 µM Ga
500 µL Ga stock 500 µL DI water 12.5 µM Ga	400 µL Ga stock 600 µL DI water 10 µM Ga	300 µL Ga stock 700 µL DI water 7.5 µM Ga	200 µL Ga stock 800 µL DI water 5 µM Ga	100 µL Ga stock 900 µL water 2.5 µM Ga	1000 µL DI water 0 µM Ga
500 µL Ga stock 500 µL DI water 12.5 µM Ga	400 µL Ga stock 600 µL DI water 10 µM Ga	300 µL Ga stock 700 µL DI water 7.5 µM Ga	200 µL Ga stock 800 µL DI water 5 µM Ga	100 µL Ga stock 900 µL water 2.5 µM Ga	1000 µL DI water 0 µM Ga
500 µL Ga stock 500 µL DI water 12.5 µM Ga	400 µL Ga stock 600 µL DI water 10 µM Ga	300 µL Ga stock 700 µL DI water 7.5 µM Ga	200 µL Ga stock 800 µL DI water 5 µM Ga	100 µL Ga stock 900 µL water 2.5 µM Ga	1000 µL DI water 0 µM Ga

<u>GaDFO CAS plate preparation</u>

Effects of Gallium-Desferrioxamine Compounds on Bacteria

Have on hand:

0.1 mM GaCl3 stock

0.1 mM DFO stock

Two 24 well plates (Falcon)

All wells: 500 µL Ga stock, 1000 µL CAS reagent mix

500 µL DFO 0 µM Ga	450 µL DFO 50 µL DI water 2.5 µM Ga	400 µL DFO 100 µL DI water 5 µM Ga	350 µL DFO 150 µL DI water 7.5 µM Ga	300 µL DFO 200 µL DI water 10 µM Ga	
500 µL DFO 0 µM Ga	450 µL DFO 50 µL DI water 2.5 µM Ga	400 µL DFO 100 µL DI water 5 µM Ga	350 µL DFO 150 µL DI water 7.5 µM Ga	300 µL DFO 200 µL DI water 10 µM Ga	
500 µL DFO 0 µM Ga	450 µL DFO 50 µL DI water 2.5 µM Ga	400 µL DFO 100 µL DI water 5 µM Ga	350 µL DFO 150 µL DI water 7.5 µM Ga	300 µL DFO 200 µL DI water 10 µM Ga	
500 µL DFO 0 µM Ga	450 µL DFO 50 µL DI water 2.5 µM Ga	400 µL DFO 100 µL DI water 5 µM Ga	350 µL DFO 150 µL DI water 7.5 µM Ga	300 µL DFO 200 µL DI water 10 µM Ga	

250 µL DFO 250 µL DI water 12.5 µM Ga	200 µL DFO 300 µL DI water 15 µM Ga	150 µL DFO 350 µL DI water 17.5 µM Ga	100 µL DFO 400 µL DI water 20 µM Ga	50 µL DFO 450 µL DI water 22.5 µM Ga	500 µL DI water 25 µM Ga
250 µL DFO 250 µL DI water 12.5 µM Ga	200 µL DFO 300 µL DI water 15 µM Ga	150 µL DFO 350 µL DI water 17.5 µM Ga	100 µL DFO 400 µL DI water 20 µM Ga	50 µL DFO 450 µL DI water 22.5 µM Ga	500 µL DI water 25 µM Ga

250 µL DFO 250 µL DI water 12.5 µM Ga	200 µL DFO 300 µL DI water 15 µM Ga	150 µL DFO 350 µL DI water 17.5 µM Ga	100 µL DFO 400 µL DI water 20 µM Ga	50 µL DFO 450 µL DI water 22.5 µM Ga	500 µL DI water 25 µM Ga
250 µL DFO 250 µL DI water 12.5 µM Ga	200 µL DFO 300 µL DI water 15 µM Ga	150 µL DFO 350 µL DI water 17.5 µM Ga	100 µL DFO 400 µL DI water 20 µM Ga	50 µL DFO 450 µL DI water 22.5 µM Ga	500 µL DI water 25 µM Ga

A3 CFU Protocol:

1. Make sure you have the following materials:
    1. fifty-four LB plates
    2. fifty-four cell spreaders
    3. seventy-two 1.5 mL microcentrifuge tubes
    4. 1 L sterile DI water
    5. 2 L 2X LB (sterile)
    6. 1 L 1X LB (sterile)
    7. 2.28×10^{-3} M GaDFO stock
    8. 2.06×10^{-3} M Ga stock
    9. eleven 250 mL autoclaved baffle flasks.
2. Obtain a sterile 250 mL Baffle flask.
3. Add 100 mL sterile 1X LB to the Baffle flask.
4. Add an entire vial of whatever bacterium you will work with (e.g. E. coli, E. aerogenes, etc) to the baffle flask with 100 mL 1X LB in it.
5. Place inoculated baffle flask in the shaker at 250 RPM and 37 °C.
6. Incubate baffle flask in the shaker until it reaches mid-log phase.
    1. For E. coli, mid log phase takes about 5 hours of incubation. O.D. for E. coli should be around 4.0.

While you wait for the culture to reach mid-log phase, the following can be done concurrently:

7. Prepare the treatment flasks.

1. There are three treatments: GaDFO treatment, Free gallium treatment, and control treatment.
2. Each treatment has three replicates.
3. Additionally, you need to set up an extra control treatment (i.e. a fourth replicate) to make a small growth curve.
4. Therefore, you should have a total of 10 treatment flasks: three GaDFO, three free gallium, and four control.

8. To make each of the treatment flasks do the following (in the hood):
    1. First, add 20 mL of 2X LB to ALL TEN baffle flasks.
    2. Next, separate the baffle flasks in to one of three groups: GaDFO, free gallium, or control.
        1. To the THREE GaDFO flasks, add 10 mL of $2.06x10^{-3}$ M sterile free gallium stock, and 10 mL of $2.28x10^{-3}$ M sterile DFO stock
        2. To the THREE Free gallium flasks, add 10 mL of $2.06x10^{-3}$ M sterile free gallium stock, and 10 mL of sterile DI water.
        3. To the FOUR Control flasks, add 20 mL of sterile DI water.
9. Prepare the dilution series in 1.5 mL centrifuge tubes.
    1. Obtain seventy two 1.5 mL centrifuge tubes, and arrange them into row of eight tubes per row.
        1. You should have nine rows of centrifuge tubes.
    2. Label the top of each individual tube with a number 1-8, and with the treatment designation (i.e. C for control, D for GaDFO, or G for free gallium), example provided below:

1C	2C	3C	4C	5C	6C	7C	8C
1C	2C	3C	4C	5C	6C	7C	8C
1C	2C	3C	4C	5C	6C	7C	8C
1D	2D	3D	4D	5D	6D	7D	8D
1D	2D	3D	4D	5D	6D	7D	8D
1D	2D	3D	4D	5D	6D	7D	8D
1G	2G	3G	4G	5G	6G	7G	8G
1G	2G	3G	4G	5G	6G	7G	8G
1G	2G	3G	4G	5G	6G	7G	8G

3. Add 900 µL of 1X LB to all 72 centrifuge tubes.

10. Prepare the plates you will use.
    1. Obtain 54 LB plates (or whatever media you need to use)
    2. Label each plate with the bacterium name, the treatment (i.e. GaDFO, free gallium, or control), the serial dilution (i.e. 10^{-3} or 10^{-4}), and the replicate number (1, 2, or 3 because there are three replicates per treatment)
    3. Place plates in the 37 °C incubator so they warm up.

Once culture reaches mid-log phase:

1. Take culture out of shaker, and measure O.D. at 600 nm wavelength. RECORD THE O.D. in the lab notebook.
    1. At this point, the culture should be very dense. Make sure you measure the O.D. using a 1:10 dilution, and the appropriate 1:10 blank.

    2. For reference, the O.D. of an E. coli culture in mid-log phase is ~4.0
2. Open the Excel sheet titled "Gemstone CFU Calculations." Enter the O.D. value you obtained next to the cell labeled "ODstart"
3. Notice the number that appears in the highlighted box. This number is the volume of cells you need to use to inoculate into EACH INDIVIDUAL TREATMENT FLASK.
    1. Note that the volume in the highlighted box is in mL. The cell next to that gives the volume in μL.
4. Record the volume of cells you will inoculate into each treatment flask.
5. Inoculate all ten treatment flasks with the appropriate volume of cells.
6. Place all ten treatment flasks in the shaker at 250 RPM and 37 °C.
7. Every ONE HOUR, take an O.D. measurement of ONE of the control flasks, and RECORD RESULTS.
    1. Remember, you should have four control flasks. Pick one of them, and take an OD from that exact same flask every hour.
    2. Make sure you take an OD of the SAME EXACT FLASK ALWAYS. This will avoid contamination of other flasks.
8. Once the control culture that you have been using to take OD measurements reaches mid-log phase, stop the shaker.
    1. Usually the O.D. at mid log phase will be around ~1.5 for E. coli. This is because you are using a smaller volume.
9. Obtain the seventy two 1.5 mL centrifuge tubes that should already be labeled, and should have 1X LB in them.
10. To the tubes labeled "1", add 100 μL of each treatment culture.

    1. You should have a total of nine tubes labeled “1”, one for each treatment flask.

11. Pipette the contents in each tube up and down at least ten times to make sure the cells are resuspended in the medium.
12. Obtain a new pipette tip, and transfer 100 µL of the contents in tube “1”, to the tubes labeled “2”.
    1. Once again, you should have a total of nine tubes labeled “2”. One for each treatment.
13. Pipette the contents in each tube up and down at least ten times to make sure the cells are resuspended in the medium.
14. Repeat steps 12 and 13 until all tubes (1-8) have cells in them. For example, the next step would be to transfer 100 µL from tube “2” to tube “3”.
    1. REMEMBER TO USE A FRESH PIPETTE TIP every time you go from tube to tube!
15. Once you have finished, tubes 1-8 should have cells in them. All 72 centrifuge tubes should also have cells.

Plating serial dilutions:

1. Obtain the 54 plates, and separate them based on the treatment (i.e. control, GaDFO, or free gallium).
2. Plate 100 µL from each microcentrifuge tube onto individual plates.
    1. Remember to resuspend the contents in the microcentrifuge tubes BEFORE pipetting contents onto plate. This will ensure that any cells that have settle come back into solution.

3. Use STERILE spreaders to spread the 100 µL around the ENTIRE Plate.
4. DO NOT turn the plates over until the 100 µL have dried on the surface of the agar.
5. Once the agar appears dry, turn plates over.
6. Leave plates in the incubator at 37 °C overnight.

Counting colony forming units:

1. Once plates have been incubated overnight, retrieve them.
2. Look for plates that appear to have between 10-100 colonies on them.
3. Count the exact number of colonies on this plate, and record the number of colonies, and the plate from which they came from.
    1. For example, 10^{-5} Control plate had 80 colonies.
4. To calculate the number of colony forming units per mL of culture, use the following formula:

$$\frac{CFU}{mL} = \frac{\#\ of\ colonies * plate\ dilution\ factor}{Volume\ of\ culture\ plated\ (mL)}$$

So, for a 10^{-6} plate with 80 colonies on it:

$$\frac{CFU}{mL} = \frac{80\ colonies * 10^{6}}{0.1\ mL}$$

Note that the dilution factor on the plate is not 10^{-6}, but 10^{6}. Also, the denominator in this equation should always be 0.1 mL because we are always going to plate 100 µL of culture onto the treatment plate.

A4 Mammalian Cell Culture Protocol:

Human Embryonic Kidney cells were supplied by the Biopharmaceutical Advancement Facility (Rockville, MD).

Cells were cultured in 1x DMEM media supplemented with 10% Fetal Bovine Serum, and 1% Penicillin/Streptomycin.

Cells were incubated at 37 °C with 5% CO_2 until their concentration reached 7,000 cells/cm^2. Cells were mixed with 10^{-2} M GaDFO stock and again incubated at 37 °C with 5% CO_2 for 20 hours with growing and confluent cells. After this incubation period, cells were counted using a hemocytometer.

Appendix B: Matlab for Microplate Fermentation Analysis

Export the fermentation data from the KC4 software such that it is reported in a single large matrix, typically six columns wide and very many rows long. This script will extract data from a 24 or 48 hour run, sampled every 15 minutes, and plot the GaDFO and DFO treatments' efficacy vs concentration.

```
plate = EAPlate120Sep14(:,2:7);
% for 48 hour plates
row1  = plate(3:195,:);
row2 = plate(198:390,:);
row3 = plate(393:585,:);
row4 = plate(588:780,:);
%for 24 hour plate
%row1  = plate(3:99,:);
%row2  = plate(102:198, :);
%row3 = plate(201:297,:);
%row4 = plate(300:396,:);
plate = [row1, row2, row3, row4];
%1:DFO 10^-2 2:DFO 10^-3 3:DFO 10^-4 4:DFO 10^-5
%5: control
%6 Ga: 10^-3 7:DFO 10^-4 8:DFO 10^-5
prefactor = 2.059*(10/38)*(19/20)
platekey = [1 1 1 2 2 2 4 4 4 3 3 3 5 5 5 6 6 6 7 7 7 8 8 8];
DFOlevels = [1 2 3 4; prefactor*10^-2 prefactor*10^-3 prefactor*10^-4
prefactor*10^-5]
Galevels = [6 7 8; prefactor*10^-3 prefactor*10^-4 prefactor*10^-5]
%A1 A2 A3 A4 A5 A6 B1 B2 etc.
truncend = 96
plate = plate(1:truncend,:)
samplet = 15
tdiff = samplet/60
tend = tdiff*length(row1)-tdiff
```

```
t = 0:tdiff:tend
t = t(1:truncend)
avgmatrix = [];
coeffmatrix = [];
for i = 1:24

       col = plate(:,i);
       xmatrix = [t'.^0 t'.^1 t'.^2 t'.^3 t'.^4];
       b = [0 0 0];
       x = zeros(96);
       x = x(:,1);
       %modelfun = @(b,x) b(1) + b(2)./(1 + exp(-x + b(3)));
       %beta0 = [.113, 0, .5];
       %X = t';
       %y = col;
       %mdl = NonLinearModel.fit(X,y,modelfun,beta0)
       %avgcol = xmatrix [193x3] * coeff [3x1]
       coeff = inv((xmatrix'*xmatrix))*xmatrix'*col;
       coeffmatrix(:,i) = coeff;
end
maxratemtrx = []
treatmentsDFO = [2*10^-2; 2*10^-3; 2*10^-4; 2*10^-5]
figure;
for i = 1:24
       model = coeffmatrix(1,i).*t.^0 + coeffmatrix(2,i).*t +
coeffmatrix(3,i).*t.^2 + coeffmatrix(4,i).*t.^3 + coeffmatrix(5,i).*t.^4
       maxrate = max(diff(model))
       maxratemtrx(i) = maxrate
       hold on
       plot(t,model, 'b')
       plot(t,plate(:,i), 'b.')
end
controlind = find(platekey == 5)
controlrates = []
for i = 1:length(controlind)
       controlrates(i) = maxratemtrx(controlind(i))
```

```
end
avgcontrolrate = mean(controlrates);
maxratemtrx = maxratemtrx./avgcontrolrate
resultmtrx = [platekey;maxratemtrx];
DFOind = find(platekey < 5);
Gaind = find(platekey > 5);
DFOresultmtrx = resultmtrx(:,DFOind);
Garesultmtrx = resultmtrx(:,Gaind);
for i = 1:length(DFOresultmtrx(1,:))
       levelindex = DFOresultmtrx(1,i);
       treatindex = find(DFOlevels(1,:) == levelindex);
       treatlevel = DFOlevels(2,treatindex);
       DFOresultmtrx(1,i) = treatlevel
end
for i = 1:length(Garesultmtrx(1,:))
       levelindex = Garesultmtrx(1,i);
       treatindex = find(Galevels(1,:) == levelindex);
       treatlevel = Galevels(2,treatindex);
       Garesultmtrx(1,i) = treatlevel
end
outDFO = [log10(DFOresultmtrx(1,:)); DFOresultmtrx(2,:)]';
outGa = [log10(Garesultmtrx(1,:)); Garesultmtrx(2,:)]';
figure;
scatter(log10(DFOresultmtrx(1,:)), DFOresultmtrx(2,:))
xlabel 'treatment level'
ylabel 'relative max growth rate'
title 'E Aero GaDFO treatments '
hold on
scatter(log10(Garesultmtrx(1,:)), Garesultmtrx(2,:), 'r')
legend('GaDFO', 'Ga')
```

Supplemental Information

S1: Amino acid sequences for DesA and *V. vulnificus* desferrioxamine B receptor.

DesA gene in *S. coelicolor.* Codes for L-2,4-diaminobutyrate decarboxylase used for making desferrioxamine E. Locus tag: SCO2782

Amino Acid Sequence:

MRSHLLNDTTAEQYRRSVTEGVERVAAKLATTDRPFTGVTVDALSPRIDA
IDLDEPLHDTAAVLDELEDVYLRDAVYFHHPRYLAHLNCPVVIPALLGEA
VLSAVNSSLDTWDQSAGGTLIERKLIDWTCARIGLGPAADGVFTSGGTQS
NLQALLLAREEAKAEDFADLRIFASEASHFSVRKSAKLLGLGPDAVVSIP
VDRDKRMQTVALARELERCARDGLVPMAVVATGGTTDFGSIDPLPEIAGL
CEQYGVWMHVDAAYGCGLLASLKYRDRITGIERADSVTVDYHKSFFQPVS
SSAVLVRDAATLRHATYHAEYLNPRRMVQERIPNQVDKSLQTTRRFDALK
LWMTLRVMGADGIGVLFDEVCDLAAEGWKLLAADPRFDVVVQPSLSTLVF
RHIPADVTDPAEIDRANLYARKALFASGDAVVAGTKVAGRHYLKFTLLNP
ETTPADIAAVLDLIAGHAEQYLGDSLDRAS

V. vulnificus Desferrioxamine B Receptor: Locus tag: VV21337

Amino Acid Sequence:

MNTTTPFKTSSIALAIMATFTTPLVAAEQSSIENAQLETTQLETITVLGK
VYRNTATKTALEPEETPQGVTIIDKELLDQRGVKSVNEALRYAPGVVTEQ
KGAAVTMYDNFSIRGFETNNQNYYDGLILPYLAGWNLHPQIDPVAIQQIE
VFKGPTSVLYGTMPPGGMVNIIAKSPQQEQSTSVGLATGSRHLVQASLDS
AGQIGDSNLSYRLVAMARKQDSQVNGADEERYLIAPSLDWQVTDRTLINV
NLYYQNDPAMGINSSMPVEVVKRQSPSVSMGDTNWSTFERDILMLGYKLN
HEFNDNWSFLQNARYTDASLYQENTYHLDTGFTAATGALSRNIYTTDESY
KSVVIDNQLSGLVTMGNWQHNLLVGVDYQDLDGDSSYKEFAGNAAFYTFN
AYQPNNNLLDKSQLNEVYSERHDIGFEQLGVYFQDQIRHGQLILLAGGRY
DLFKSHDDKTSTAPTYDGKETSDHNQFSYRVGALYELGNGLSPFANYATS
FEPAAGTDINGKSLKPQTGEQIEVGFKYMSADMANTLTASYFNITKFDSI
AADPNDPTFRAKIQLGEVTSQGVELEGQAYLADNWDVLASYTYLDMEVKK
ATDATLVGTTPIYVPKHSANLWTNYYLTSGALSGARIGGGVRYVGEMEMD
ATNTQGKVPSYTVADLSLGYDLGSASDSLNGAQVNLVVNNLFNEQYYSCY
NQTNCWFGAEQTVELNVNYGF

S2: List of Gram Negative Pathogens Evaluated for DesA and Receptor Homology

Genus	Species
Bordetella	*Pertussis*
Borrelia	*Burgdorferi*
Brucella	*Suis*
Campylobacter	*Jejuni*
Francisella	*Tularensis*
Haemophilus	*Influenzae*
Helicobacter	*Pylori*
Legionella	*Pneumophila*
Neisseria	*Gonorrhoeae*
	Meningitidis
Pseudomonas	*Aeruginosa*
Salmonella	*Typhi*
	Typhimurium
Shigella	*Sonnei*
Treponema	*Pallidum*
Vibrio	*Cholerae*
Yersinia	*Pestis*

S3: List of Treatment Concentrations

Reported Concentration	Log10(Reported Concentration)	[Ga] (M)	[DFO] (M)	[Ga] (g/L)	[DFO] (g/L)	Ga/DFO ratio
5.15E-003	-2.29E+000	5.15E-003	5.72E-003	3.59E-001	3.76E+000	0.9
5.15E-004	-3.29E+000	5.15E-004	5.72E-004	3.59E-002	3.76E-001	0.9
5.15E-005	-4.29E+000	5.15E-005	5.72E-005	3.59E-003	3.76E-002	0.9
5.15E-006	-5.29E+000	5.15E-006	5.72E-006	3.59E-004	3.76E-003	0.9

Reported Concentration	Log10(Reported Concentration)	[Ga] (M)	[Ga] (g/L)
5.15E-003	-2.29E+000	5.15E-003	3.59E-001
5.15E-004	-3.29E+000	5.15E-004	3.59E-002
5.15E-005	-4.29E+000	5.15E-005	3.59E-003
5.15E-006	-5.29E+000	5.15E-006	3.59E-004